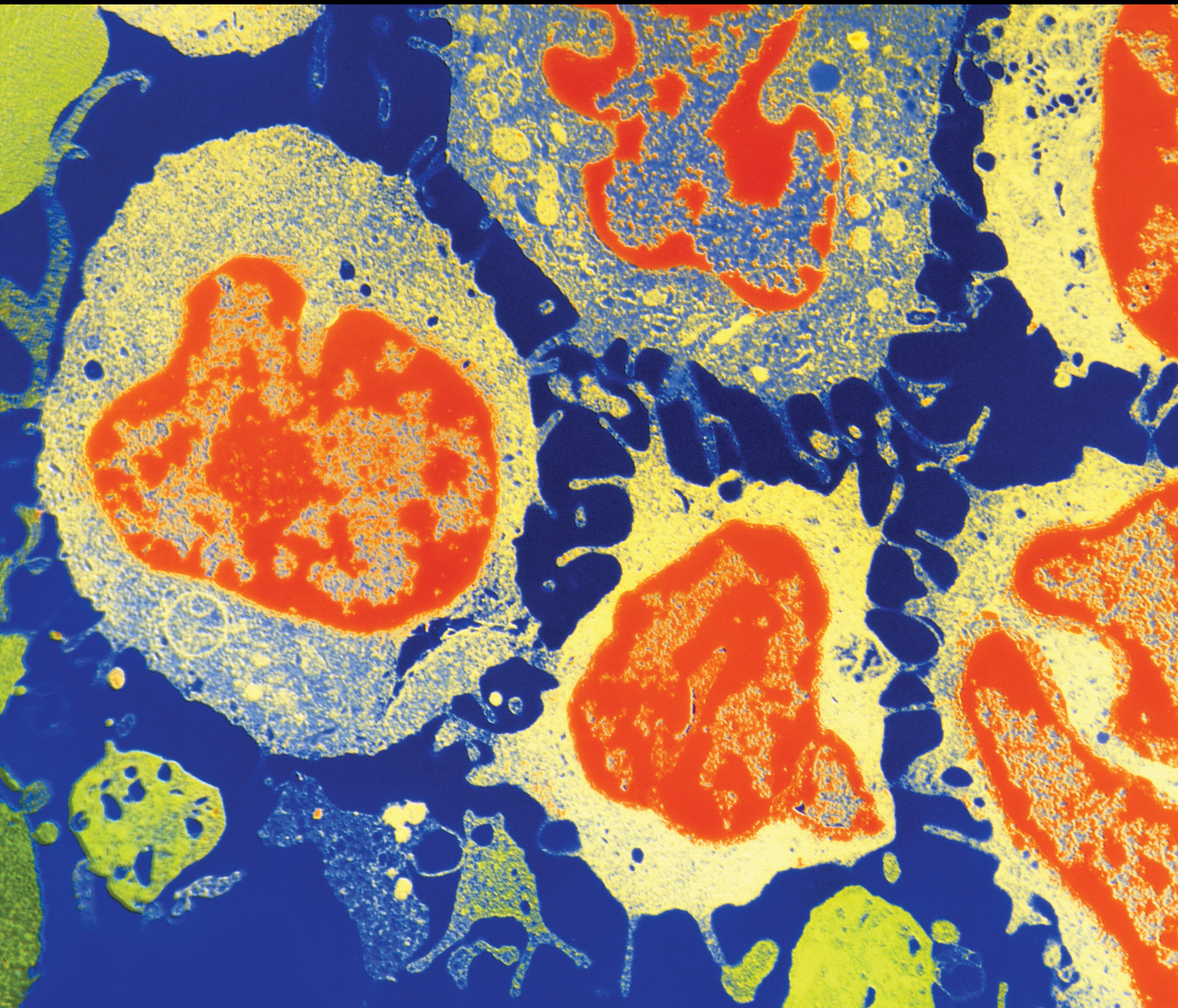


Emerging Topics in Orthopaedic Oncology

Lead Guest Editor: Said Saghieh

Guest Editors: Ahmad Shehadeh and Michelle Ghert





Emerging Topics in Orthopaedic Oncology

Journal of Oncology

Emerging Topics in Orthopaedic Oncology

Lead Guest Editor: Said Saghieh

Guest Editors: Ahmad Shehadeh and Michelle
Ghert



Copyright © 2020 Hindawi Limited. All rights reserved.

This is a special issue published in "Journal of Oncology" All articles are open access articles distributed under the Creative Commons Attribution License, which permits unrestricted use, distribution, and reproduction in any medium, provided the original work is properly cited.

Chief Editor

Bruno Vincenzi, Italy

Academic Editors

Thomas E. Adrian, United Arab Emirates

Ruhai Bai , China

Jiaolin Bao, China

Rossana Berardi, Italy

Benedetta Bussolati, Italy

Sumanta Chatterjee, USA

Thomas R. Chauncey, USA

Gagan Chhabra, USA

Francesca De Felice , Italy

Giuseppe Di Lorenzo, Italy

Xiangya Ding , China

Peixin Dong , Japan

Xingrong Du, China

Elizabeth R. Dudnik , Israel

Pierfrancesco Franco , Italy

Ferdinand Frauscher , Austria

Rohit Gundamaraju, USA

Han Han , USA

Jitti Hanprasertpong , Thailand

Yongzhong Hou , China

Wan-Ming Hu , China

Jialiang Hui, China

Akira Iyoda , Japan

Reza Izadpanah , USA

Kaiser Jamil , India

Shuang-zheng Jia , China

Ozkan Kanat , Turkey

Zhijia Kang , USA

Pashtoon M. Kasi , USA

Jorg Kleeff, United Kingdom

Jayaprakash Kolla, Czech Republic

Goo Lee , USA

Peter F. Lenehan, USA

Da Li , China

Rui Liao , China

Rengyun Liu , China

Alexander V. Louie, Canada

Weiren Luo , China

Cristina Magi-Galluzzi , USA

Kanjoormana A. Manu, Singapore

Riccardo Masetti , Italy

Ian E. McCutcheon , USA

Zubing Mei, China

Giuseppe Maria Milano , Italy

Nabiha Missaoui , Tunisia

Shinji Miwa , Japan

Sakthivel Muniyan , USA

Magesh Muthu , USA

Nandakumar Natarajan , USA

P. Neven, Belgium

Patrick Neven, Belgium

Marco Noventa, Italy

Liren Qian , China

Shuanglin Qin , China

Dongfeng Qu , USA

Amir Radfar , USA

Antonio Raffone , Italy

Achuthan Chathrattil Raghavamenon, India

Faisal Raza, China

Giandomenico Roviello , Italy

Subhadeep Roy , India

Prasannakumar Santhekadur , India

Chandra K. Singh , USA

Yingming Sun , China

Mohammad Tarique , USA

Federica Tomao , Italy

Vincenzo Tombolini , Italy

Maria S. Tretiakova, USA

Abhishek Tyagi , USA

Satoshi Wada , Japan

Chen Wang, China

Xiaosheng Wang , China

Guangzhen Wu , China

Haigang Wu , China

Yuan Seng Wu , Malaysia

Yingkun Xu , China

WU Xue-liang , China

ZENG JIE YE , China

Guan-Jun Yang , China

Junmin Zhang , China

Dan Zhao , USA

Dali Zheng , China

Contents

FAM64A Promotes Osteosarcoma Cell Growth and Metastasis and Is Mediated by miR-493

Ying Jiang, Chunlei Zhou, Qiang Gao, Zhi-Qi Yin, Jingwen Wang, Hong Mu, and Jun Yan 

Research Article (13 pages), Article ID 2518297, Volume 2020 (2020)

Surgical Technique and Outcome of Custom Joint-Sparing Endoprosthesis as a Reconstructive Modality in Juxta-Articular Bone Sarcoma

Ahmad M. Shehadeh , Ula Isleem , Samer Abdelal, Hamza Salameh , and Muthana Abdelhalim

Research Article (13 pages), Article ID 9417284, Volume 2019 (2019)

Research Article

FAM64A Promotes Osteosarcoma Cell Growth and Metastasis and Is Mediated by miR-493

Ying Jiang,¹ Chunlei Zhou,¹ Qiang Gao,¹ Zhi-Qi Yin,² Jingwen Wang,² Hong Mu,¹ and Jun Yan ²

¹Department of Clinical Laboratory, Tianjin First Center Hospital, Tianjin 300192, China

²Department of Pathology, Tianjin First Center Hospital, Tianjin 300192, China

Correspondence should be addressed to Jun Yan; yanhuang2@163.com

Received 9 August 2019; Revised 20 January 2020; Accepted 28 January 2020; Published 24 February 2020

Academic Editor: Michelle Ghert

Copyright © 2020 Ying Jiang et al. This is an open access article distributed under the Creative Commons Attribution License, which permits unrestricted use, distribution, and reproduction in any medium, provided the original work is properly cited.

Aberrant expression of FAM64A was correlated with cell proliferation in various cancer types. We examined the expression of FAM64A and the upstream gene miR-493 in OS. The functions of miR-493 were revealed through extensive experiments. We found an increase of FAM64A gene and protein in OS tissues. Overexpression of FAM64A resulted in promoting tumor proliferation, migration, and invasion. The miR-493 targeted and negatively regulated FAM64A. Our data showed that upregulation of FAM64A in OS correlated with poor prognosis.

1. Introduction

Osteosarcomas are originated from primitive mesenchymal cells and defined as the most prevalent primary solid tumor of the bone. Due to the heterogeneity of osteosarcoma, the etiology of OS in most patients is still obscure. Fletcher et al. determined increased incidence of OS in cases with altered tumor suppressor genes [1]. For example, CATS (FAM64A) is confirmed to be highly expressed in leukemia, lymphoma, and a range of tumor cell lines. Moreover, it has been reported that its protein levels have intense relationship with proliferation in both tumor cells and nonmalignant cells. Silencing of FAM64A resulted in decreased proliferation and cell cycle progression of hematopoietic cells [2]. However, the research of FAM64A is inadequate; thus, the role of FAM64A in OS cells is still poorly understood.

The dysregulation of intracellular signaling pathways such as Notch1, Akt, Wnt pathway, and JAK2/STAT3 was reported to be participated in the development of OS [3–6]. Xu et al. found that FAM64A served as a positive regulator of STAT3, which is linked to various cancer types [7]. Here, we tried to find a new mechanism that interacts with FAM64A in OS. In this study, we provide an insight into the

expression patterns of genes in OS and control samples. We identified the genomic aberrations and the molecular mechanism associated with OS. We discovered the tumor-derived miR-493 targeted to FAM64A and regulated the cell growth and metastasis of OS.

2. Materials and Methods

2.1. Genomic Data of OS. From Gene Expression Omnibus (GEO; available at <http://www.ncbi.nlm.nih.gov/geo/>) database, we retrieved the gene expression profiling of OS. The keywords including *Homo sapiens* and OS were used. The informatics analysis of FAM64A levels in OS was performed in the Cancer Genome Atlas (TCGA) database.

2.2. Clinical Specimens. From May 2016 to May 2019, 30 patients in total including 17 males and 13 females (average age: 29 years, range: 19 to 46 years) diagnosed with spinal osteosarcoma were included in this study at our hospital (China). All the patients in this study have not received any type of treatment before surgery. Tumor tissues and adjacent normal tissues from patients were stored at -80°C . The

protocol for this study was approved by the Ethics Committee at our local institution.

2.3. Cell Lines. Human osteosarcoma MG63, U-20S cells, and 293T cells were purchased from FuHeng Cell Center, Shanghai, China. Cells were cultured in DMEM (Dulbecco's modified Eagle's medium, Gibco, Life Technologies) containing 10% (v/v) fetal bovine serum (Gibco, Life Technologies) at 37°C in a humidity incubator with 5% CO₂.

2.4. Xenograft Model of Tumor. For the xenograft tumor model, 1×10^7 U937 MG-63-Scramble/MG-63-siFAM64A transfected cells were implanted into the 12-week-old C57BL/6 mice. Tumor was measured after tumor cells were injected for 2 weeks.

2.5. Cell Transfection. The plasmid used was pCDH-CMV-MCS-EF1-Puro. The miR-493 mimics and negative control (miR-NC) were purchased from Shanghai GenePharma (China). After the tumor cells were grown into 75% confluence in 6-well plates, miR-493 mimics (100 pmol) and miR-NC (100 pmol) were used for transfection with the help of Lipofectamine 2000 (Invitrogen; Thermo Fisher Scientific).

2.6. Cell Viability Assay. OS cell viability was measured with A CCK-8 assay (Dojindo Molecular Technologies, Japan). Specifically, cells with a density of 7,000 cells/well were firstly seeded in 96-well plates. After 6 h of culture, cells were transfected with MG-63-NC, MG-63-FAM64, U-2 OS-NC, and U-2 OS-FAM64A, respectively, and then incubated at 37°C with 5% CO₂ for 0, 24, 48, and 72 h, respectively. At each time-point, a CCK-8 reagent of 10 μ l was added into each well, and the incubation was subsequently extended for an additional 2 h at 37°C. The absorbance of each well was measured with a microreader (Bio-Rad, USA) at 450 nm.

2.7. Cell Invasion Assay. The invasiveness of OS cells was measured with a Transwell assay using Transwell chambers (8 μ m, Corning) preburden Matrigel (BD, USA). In detail, cells were first collected and then resuspended in the FBS-free culture medium at a density of 2×10^5 cells/ml. After that, the upper chambers were then seeded with 200 μ l cell suspension, while the lower chambers were filled with 600 μ l DMEM containing 10% FBS. Following a further incubation for 48 h at 37°C, the noninvasive cells were removed by cotton-tipped swabs. Images of invasive cells were taken, and the number was counted under Nikon ECLIPSE TS100 (Nikon) at $\times 100$ magnification.

2.8. Dual-Luciferase Activity Assay. PCR was used to amplify the 3'UTR of FAM64A containing the potential miR-493 binding site. 293T cells were then cotransfected with NC/494 mimics and psiCHECK2-FAM64A3-UTR WT/psiCHECK2-FAM64A3-UTR MT. The dual-luciferase reporter

assay (Promega) was then used to measure the relative luciferase activity.

2.9. Q-RT-PCR. The total RNA from tissues and cells was isolated with TRIzol (Thermo Fisher Scientific, Inc.). In terms of miR-493, U6 was used as an internal reference. Following the synthesis of cDNA using a TaqMan MicroRNA Reverse Transcription kit (Applied Biosystems; Thermo Fisher Scientific, Inc.), PCR was then carried out with the TaqMan MicroRNA PCR kit (Applied Biosystems; Thermo Fisher Scientific, Inc.). The primers used in this study were as follows: miR-493 forward, 5'-TTGTACATGGTAGGCTTTCATT-3' and reverse 5'-AACCATTTATTTCTCCCGACC-3; U6 forward, 5'-GCTTCGGCAGCACATATACTAAAAT-3' and reverse 5'-CGCTTCACGAATTTGCGTGTTCAT3'; FAM64A forward, 5'-CCTGGAAACGCCTGGAAAC-3' and reverse 5'-CAAAGCACTCTTAGCTGAGCG-3'. The $2^{-\Delta\Delta Cq}$ method was used to determine the expression level of miR-493 and FAM64A.

2.10. Western Blot Analysis. Cellular lysates were electrophoresed in a 10% SDS-PAGE gel and then transferred to nitrocellulose membrane (GE Healthcare). Primary antibody anti-CATS 2C4 (1:1000) and GAPDH were purchased from Abcam. The membranes were rinsed with TBS (Tris-Buffered Saline) and Tween (Sigma-Aldrich) twice before being incubated with Goat Antimouse IgG H&L (HRP) for 1 h at room temperature in the dark. A Bio-Rad ChemiDoc™ XRS system was then used for membrane visualization.

2.11. Wound Healing Assay. The cells with a density of 8×10^4 cells/well were seeded in a 24-well plate. A vertical line was drawn among them with a sterile pipette tip after approximately 80% of the confluency was reached. The suspended single cells on the surface were then washed away with warm PBS. Fresh DMEM containing 10% FBS was added to plates, and the cells were then cultured in an incubator at 37°C with 5% CO₂. The cells were imaged under a phase contrast light microscope, at 0, 24, and 48 h, respectively. Cells' migration ability was then measured with Image J (National Institutes of Health).

2.12. Statistical Analysis. All data in this study were expressed as mean \pm SD (standard deviation). SPSS 22.0 was used throughout this study for the statistical analysis, and one-way analysis of variance was used for comparison. Survival of mice in this study was measured with Kaplan–Meier analysis. A $P < 0.05$ was designated as statistically significant.

3. Results

3.1. Overexpression of FAM64A in OS Tissues Predicted Poor Prognosis. As shown in Figure 1(a), GSE12865 and GSE28425 were selected on GEO to select differentially expressed genes, with $P < 0.05$ and logFC absolute value > 1.5 . There were 1,504 GSE28425 differentially screened

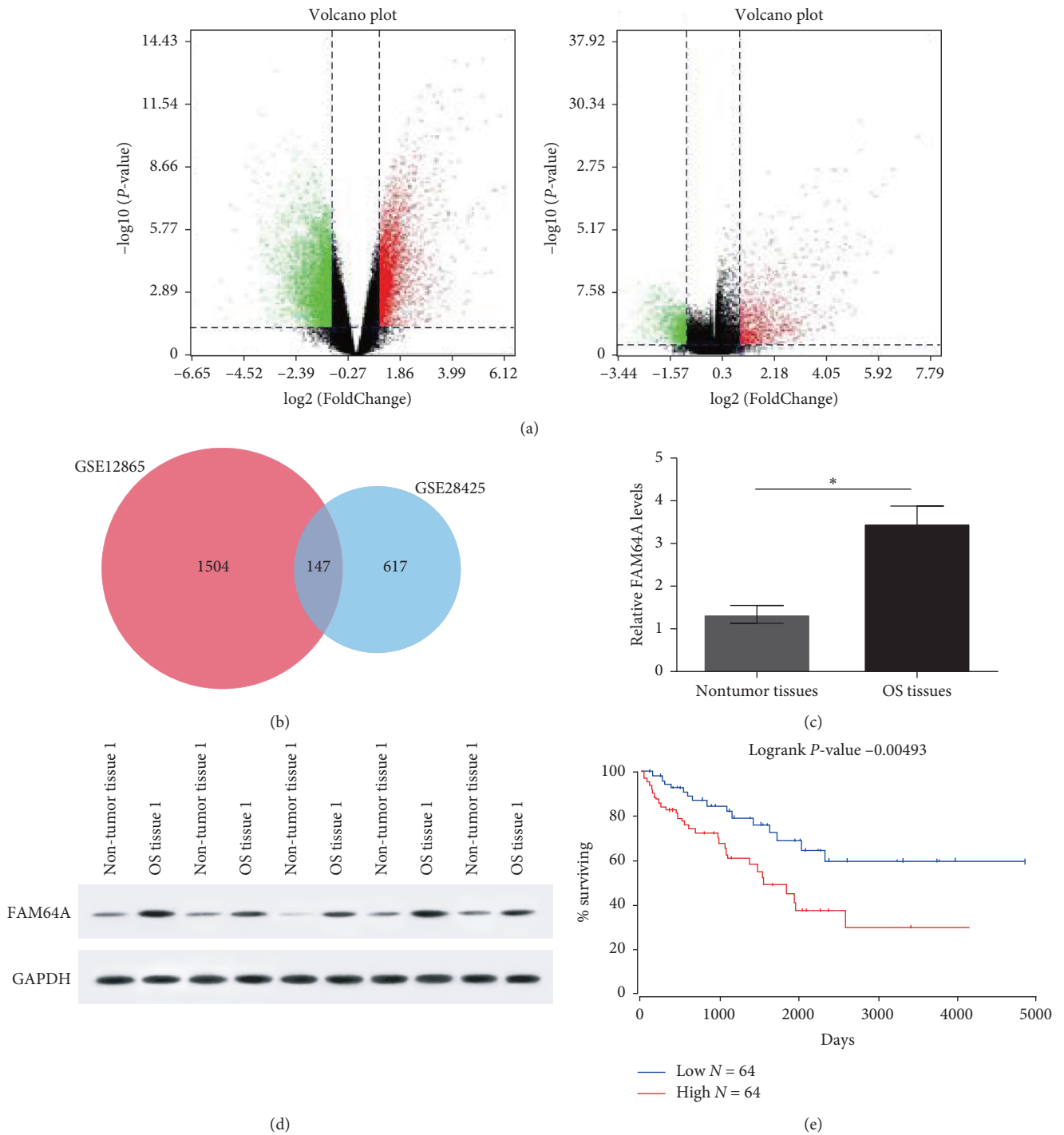


FIGURE 1: Expression of FAM64A in tumor tissues. (a) Differentially expressed genes were selected on GEO. (b) A total of 147 genes were obtained. (c) Gene expression of FAM64A in OS tissues and nontumor tissues using RT-PCR. (d) Protein expression of FAM64A in 5 pairs subject using western blot. (e) Kaplan plot for FAM64A in SARC. * $P < 0.05$. OS, osteosarcoma.

genes GSE12865 and 617 intersections, and a total of 147 genes were obtained (Figure 1(b)). The expression level of FAM64A in OS tissues and adjacent nontumor tissues were analyzed. As demonstrated in Figures 1(c) and 1(d), the gene expression level of FAM64A and its protein in tumor tissues were significantly heightened compared with the control sample ($P < 0.05$). To GO annotate these 147 genes, we

focused on this FAM64A. GO: 0009987 cellular processes. Online software (<http://www.oncolnc.org>) was used to analyze the SARC data of TCGA, and it was found that the difference of KM curve logrank analysis between patients with high and low expression of this gene, suggesting patients with higher expression of FAM64A, had poor outcome (Figure 1(e)).

3.2. Overexpression of FAM64A Promoted Proliferation, Migration, and Invasion of OS Cells. To further investigate the role of FAM64A in OS, OS cells were transfected with plasmid. The data of western blot confirmed that FAM64A was significantly upregulated in MG-63 and U-2 OS cells (Figures 2(a) and 2(b), $P < 0.05$). The CCK-8 assay and Transwell invasion assay were performed to verify the influence of overexpression of FAM64A on OS cell proliferation and invasion. As shown in Figures 2(c) and 2(d), MG-63 and U-2 OS cells transfected with FAM64A had a significantly higher proliferation rate than cells transfected with vector ($P < 0.05$). Migration assay demonstrated that the migrated numbers of MG-63 and U2OS cells transfected with FAM64A were significantly higher compared with the cells transfected with vector (Figures 2(e) and 2(f); $P < 0.05$). Additionally, invasion assay indicated that invasive abilities were markedly heightened in MG-63 and U2OS cells transfected with FAM64A plasmid (Figures 2(g) and 2(h); $P < 0.05$).

3.3. Silencing FAM64A Inhibited Proliferation, Migration, and Invasion of OS. To verify the mode of action of FAM64A, siRNA was utilized to downregulate its expression in mg-63 and U-2 OS cells (Figures 3(a) and 3(b), $P < 0.05$). The introduction of FAM64A siRNA into MG-63 and U-2 OS cells resulted in impeded tumor cell proliferation (Figures 3(c) and 3(d); $P < 0.05$), migration (Figures 3(e) and 3(f); $P < 0.05$), and invasion (Figures 3(g) and 3(h); $P < 0.05$), compared with the Scramble group.

3.4. Silencing FAM64A in Mice Inhibited OS Tumor Growth. We explored the regulatory effects of FAM64A in vivo. As displayed in Figures 4(a) and 4(b), si-FAM64A treatment significantly decreased the volume of tumor and its weight compared with the Scramble group ($P < 0.05$). The Kaplan–Meier survivor function revealed that Silencing FAM64A significantly improved the survival of tumor-bearing mice (Figure 4(c), $P < 0.05$).

3.5. FAM64A Is the Target of miR-493. Through bioinformatics analysis, we found that many miRNAs may regulate FAM64A. MiR-493 has been proved to play the role of tumor suppressor gene in osteosarcoma and inhibit the cell biological process of osteosarcoma, playing an opposite role with FAM64A [8, 9]. So, we chose miR-493 to study its regulation on FAM64A expression. Our data showed that contains a potential complimentary binding site for miR-493 within FAM64A 3'-UTR (Figure 5(a)). The possible participation of miR-493 in the FAM64A pathway is indicated in Figure 5(b). The data of luciferase activity showed that luciferase activities were significantly decreased in 293T cells after transfection with psiCHECK2-FAM64A 3'-UTR WT and miR-493 mimics (Figure 5(c), $P < 0.05$). We also analyzed the levels of FAM64A in MG-63 and U-2 OS cells transfected with miR-493 mimics, inhibitor or NC. 48 h after transfection, gene expression at mRNA levels were measured with real-time PCR. As demonstrated in Figures 5(d) and 5(e), FAM64A mRNA levels were significantly alleviated in mimics, while FAM64A mRNA levels

were increased when burden inhibitor (both $P < 0.05$). The effect of mimics was suppressed by MT, suggesting miR-493 targeting to FAM64A 3'-UTR. We also showed that miR-493 expressions were downregulated in OS tissues and negatively correlated with FAM64A mRNA expressions (Figures 5(f) and 5(g), $P < 0.05$).

3.6. MiR-493 Inhibits Proliferation, Migration, and Invasion of OS Cells via Regulating FAM64A. To investigate the role of miR-493/FAM64A in OS, OS cells were transfected with miR-493 mimics and miR-493 inhibitors with FAM64A plasmids and FAM64A siRNAs. The CCK-8 assay, wound healing assay and Transwell invasion assay were performed to investigate the proliferation, migration, and invasion. The results suggested that miR-493 significantly influenced the proliferation (Figures 6(a)–6(d)), migration (Figures 6(e)–6(j)), and invasion (Figures 6(k)–6(p)) of MG-63 and U-2 OS cells, while FAM64A plasmids and FAM64A siRNAs could attenuate the effects of miR-493 mimics and miR-493 inhibitors, respectively (Figures 6(a)–6(p)). These assays demonstrated that miR-493 inhibited proliferation, migration, and invasion of OS cells via regulating FAM64A.

4. Discussion

Recent studies have shown that FAM64A, also named as CATS and PIMREG, participates in malignant transformation [10–13]. FAM64A was first studied in hematologic carcinomas, which was known as CALM/AF10 interacting proteins. As reported, higher levels of FAM64A was associated with the tumor proliferation process. However, the role of FAM64A in solid tumor is still few. Here, we evaluated the gene expression profiling of OS in the database and found the FAM64A. Based on the data from GEO, we chose FAM64A and evaluated its expression in tumor samples. We found elevated expression of FAM64A in tumor tissues in comparison to the nontumor tissues.

Moreover, we identified the promotion of tumorigenicity by establishing overexpressing FAM64A OS cells model, which indicated underlying molecular mechanism of how miR-493 participated in upregulating migration and invasion of tumor cells. Previous evidence suggested that miR-493 inhibits the biological behavior of lung tumor [14]. Meanwhile, miR-493 also acts as a suppressor in various cancers including colon cancer, bladder cancer, and ovarian cancer via multiple intracellular signaling pathways [15–17].

Next, we performed a xenograft model of tumor and further investigated the prognostic role of FAM64A in mice. We found a sharp decrease of tumor volume and tumor weight in siRNA-transfected mice, indicating silencing FAM64A suppressed tumor growth. Kaplan–Meier curves for OS *in vivo* revealed that upregulation of FAM64A was positively correlated with worse outcomes. To confirm the interaction of FAM64A and miR-493, we performed the luciferase reporter assay. The effects of FAM64A knockdown on OS cells mimicked those induced by miR-493 mimics and were reversed by miR-493 inhibitor.

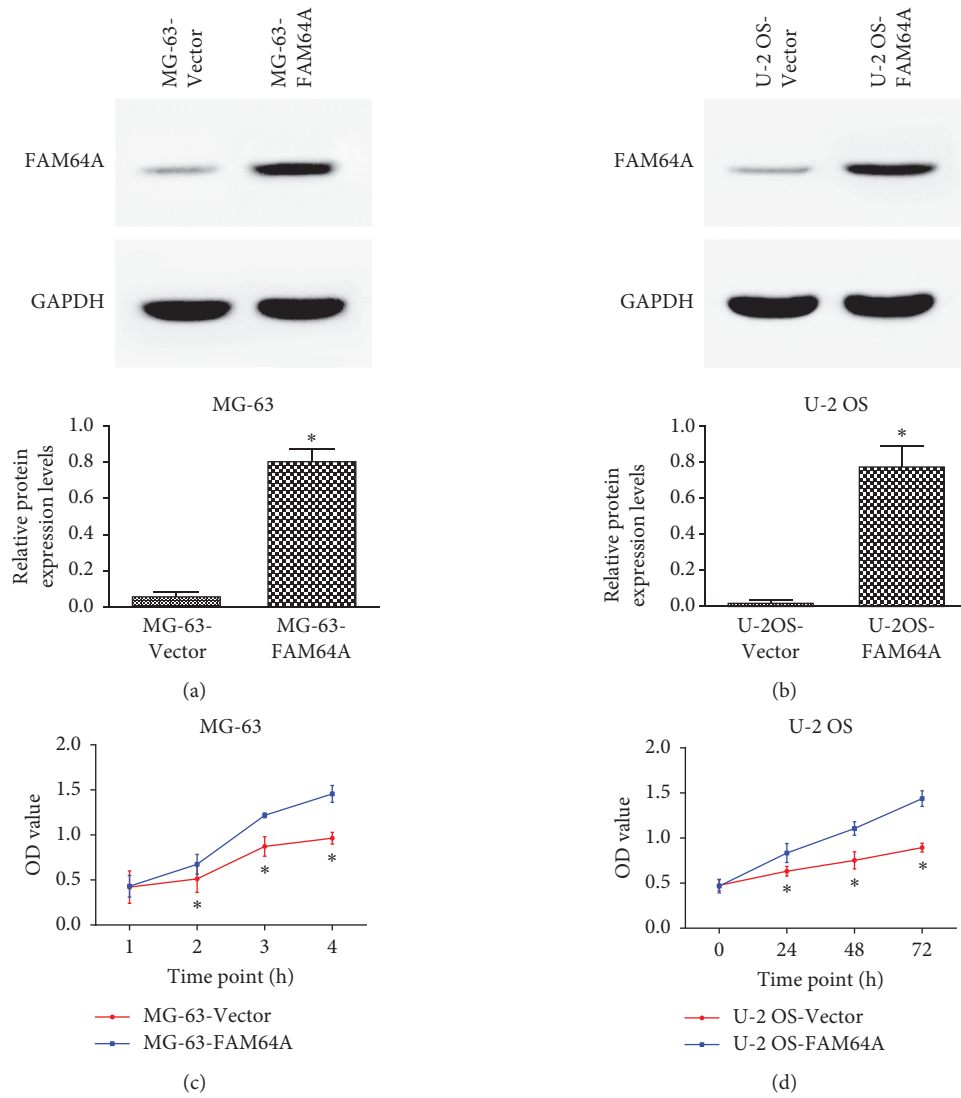


FIGURE 2: Continued.

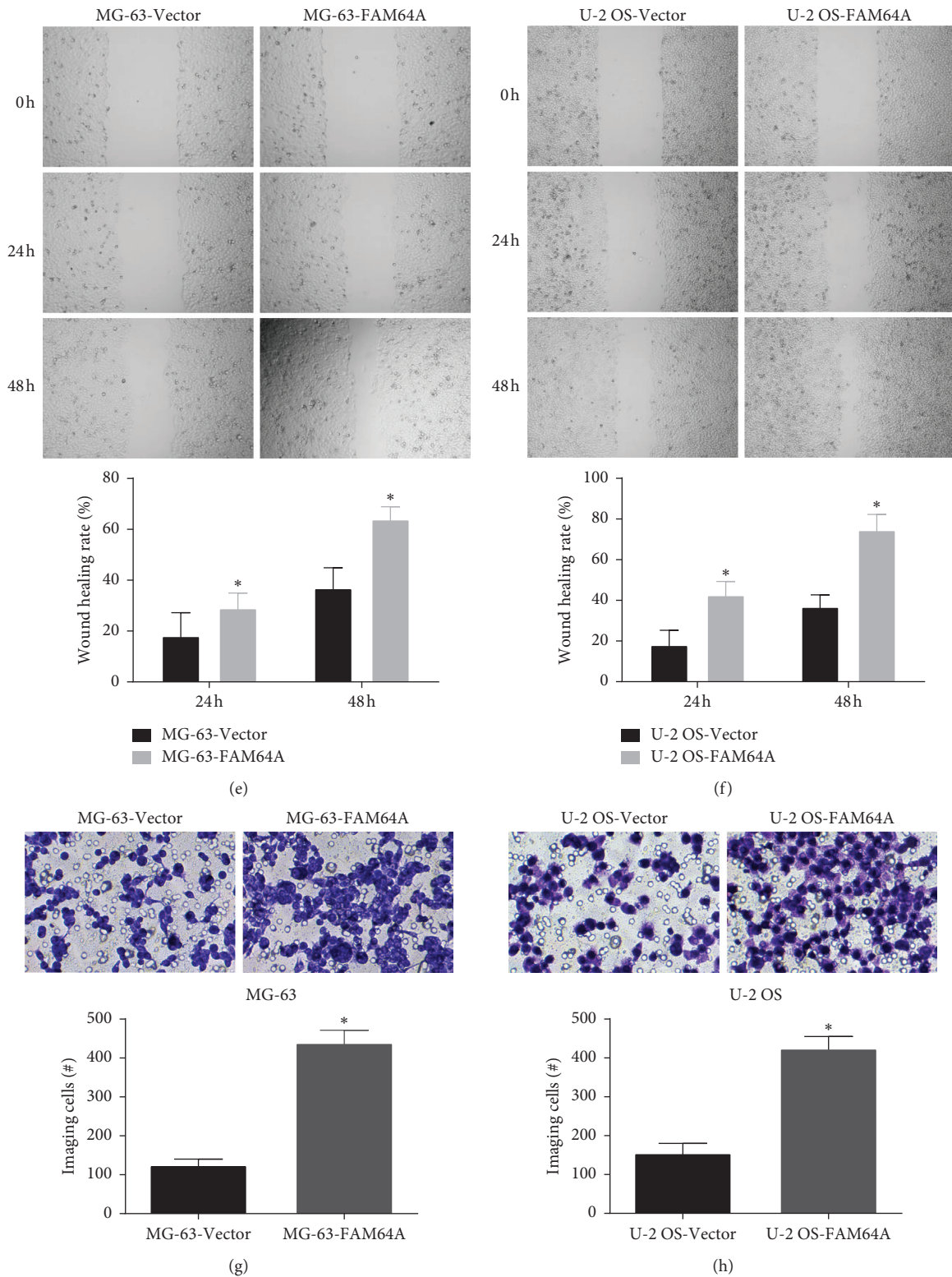


FIGURE 2: Upregulation of FAM64A promoted the tumorigenicity of OS cells. (a) and (b) Protein expression of FAM64A was detected after vector and FAM64A plasmid transfection. (c) and (d) Proliferation of tumor cells was determined by CCK-8 assay. (e) and (f) Migration was measured by the wound healing assay. (g) and (h) Invasion of cells was analyzed using a Transwell assay. * $P < 0.05$.

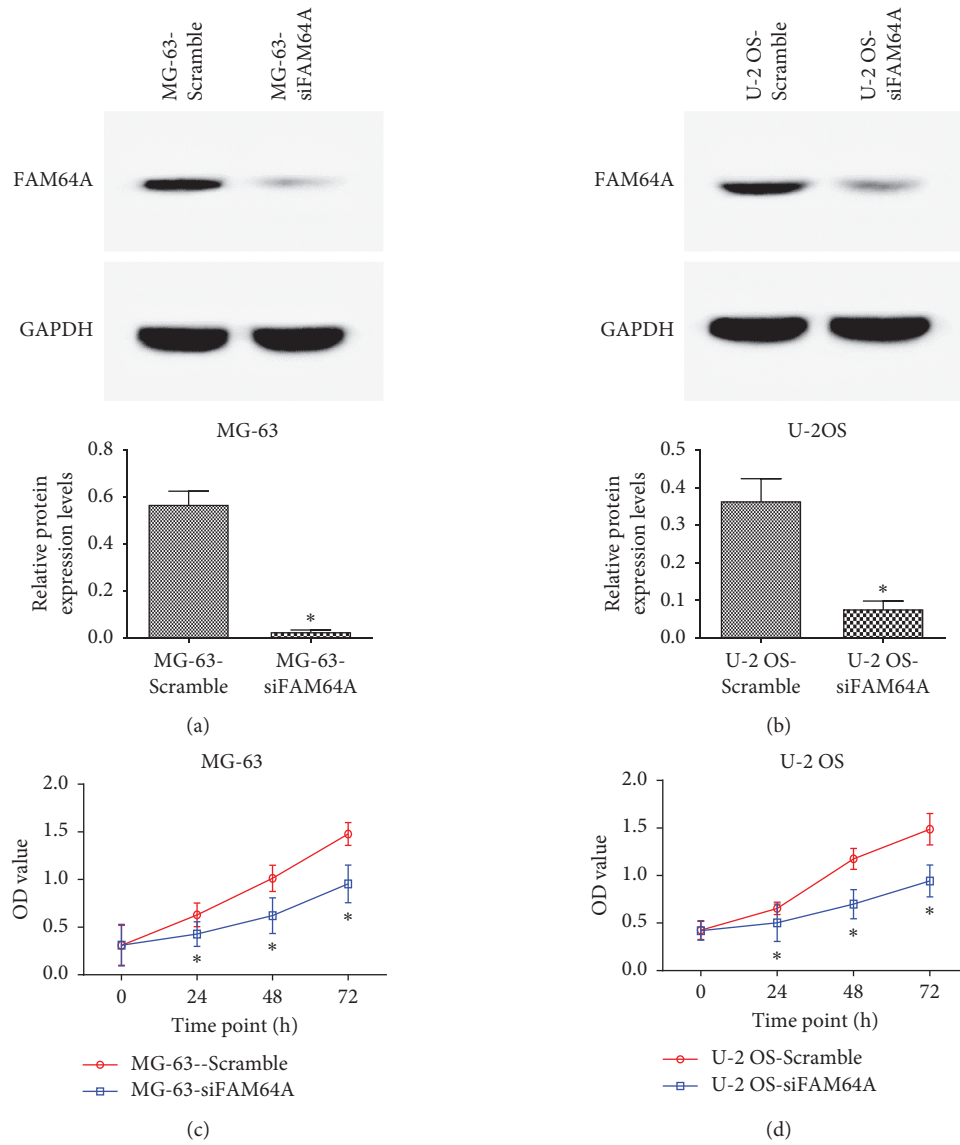


FIGURE 3: Continued.

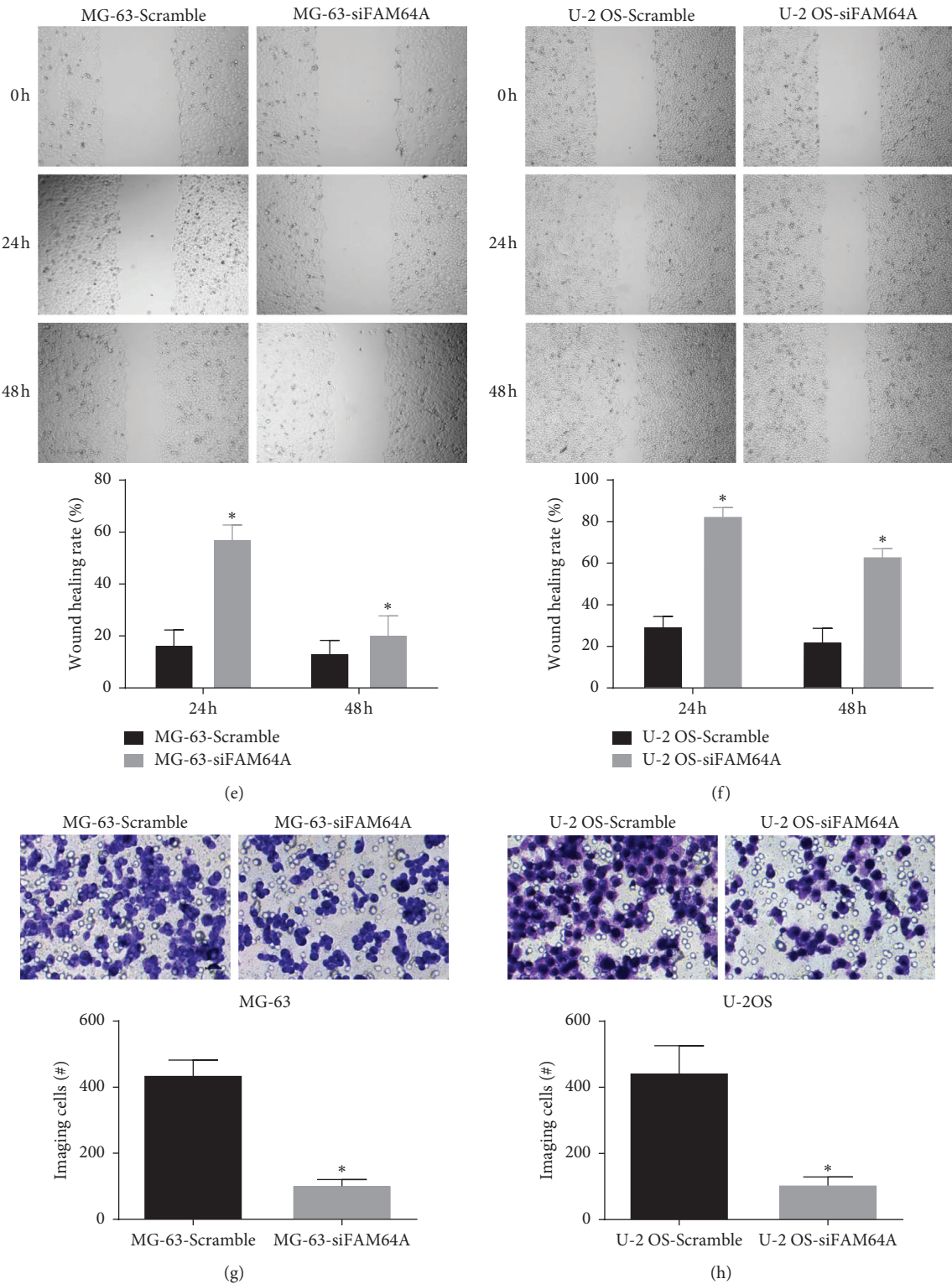


FIGURE 3: Functional effects of FAM64A siRNA knockdown on MG-63 and U-2 OS cells. (a) Protein expressions of FAM64A in si-control and si-FAM64A transfected cells. (g) and (h) migration assay of si-FAM64A transfectants. Representative photomicrographs are shown at 100 magnification.

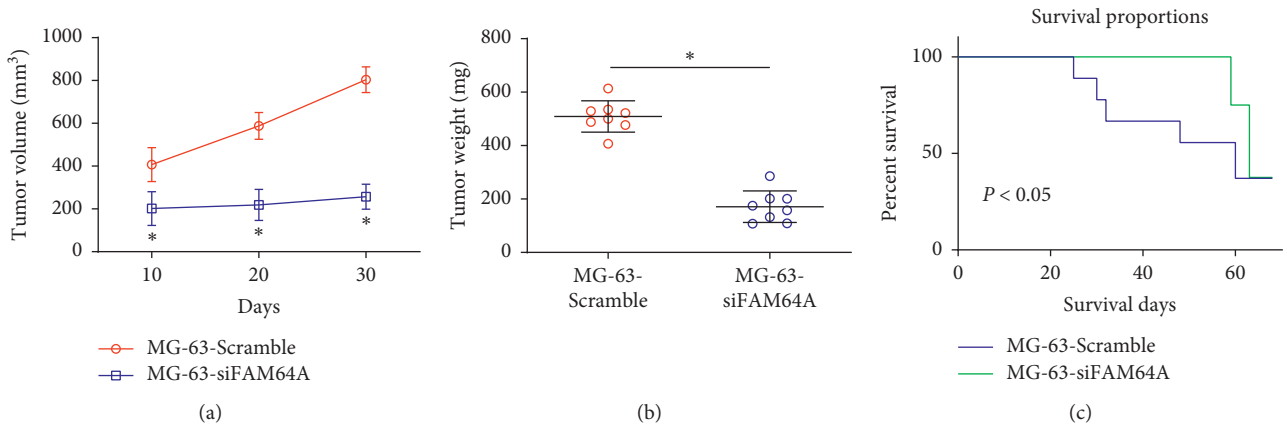


FIGURE 4: Silencing FAM64A in mice. (a) Tumor volume of mice burden MG-63-Scramble/MG-63-siFAM64A cells was measured at 10, 20, and 30 days. (b) Mice were sacrificed after 30 days, and tumor weight of mice burden MG-63-Scramble/MG-63-siFAM64A cells was analyzed. (c) Survival rate of mice. **P* < 0.05.

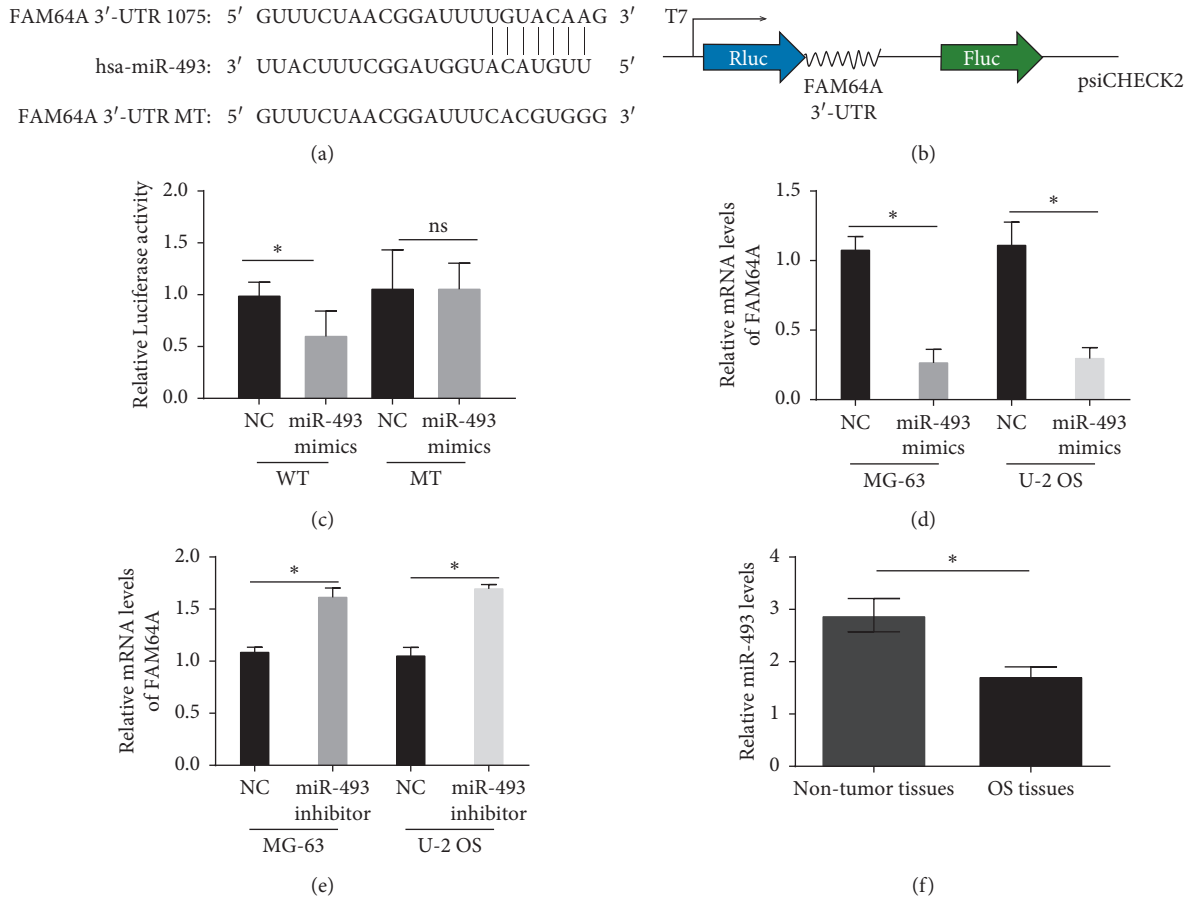


FIGURE 5: Continued.

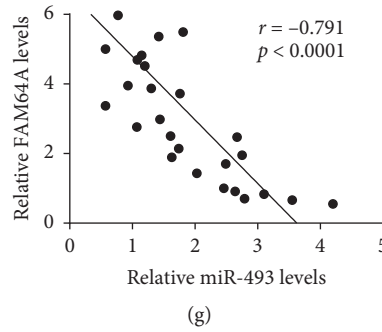


FIGURE 5: FAM64A is the target of miR-493 in OS. (a) MiR493 binding sequence in 3'UTR of the FAM64A gene and the mutant sequence. (b) The pattern of FAM64A 3-UTR WT/MT inserted to psiCHECK2. (c) 293T cells were cotransfected with psiCHECK2-FAM64A 3'-UTR WT or psiCHECK2-FAM64A 3'-UTR MT and miR493 mimics or NC. The luciferase activity was measured. (d) and (e) mRNA levels of FAM64A in MG-63 and U-2 OS cells. (f) Detection of miR-493 expressions in OS tissues and nontumor tissues using RT-RCR; (g) correlation analysis of miR-493 levels with FAM64A mRNA levels. **P* < 0.05. UTR: untranslated region; WT: wild type; MT: mutant; NC: negative control.

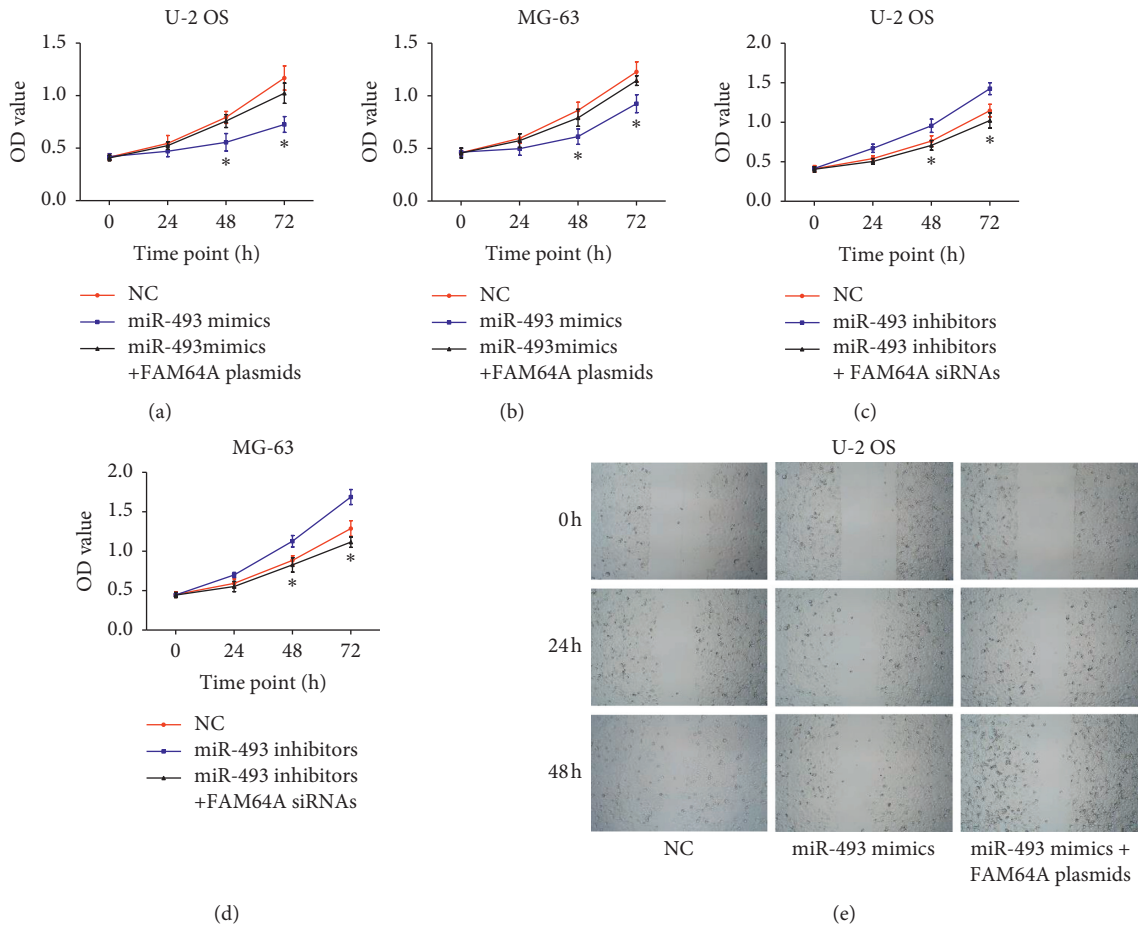
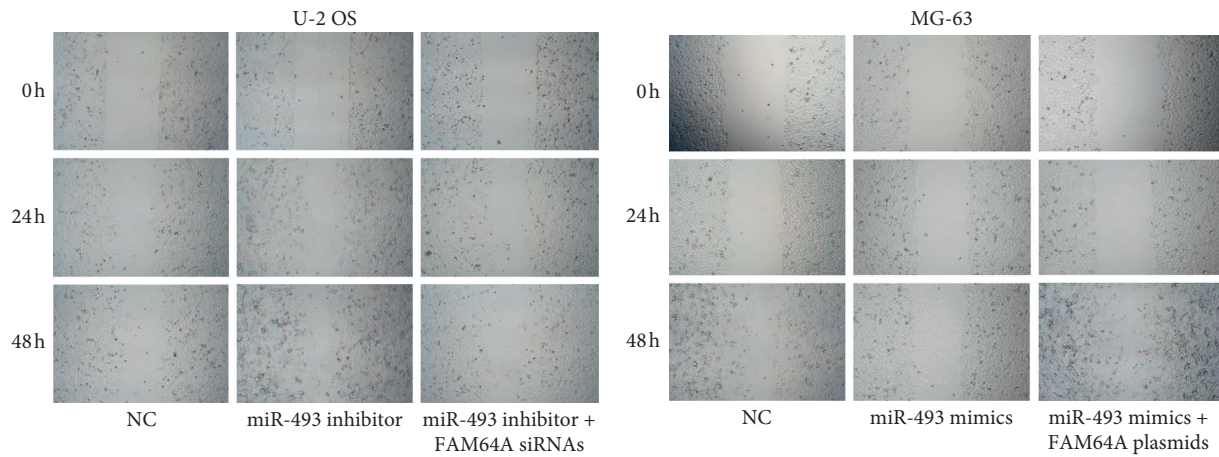
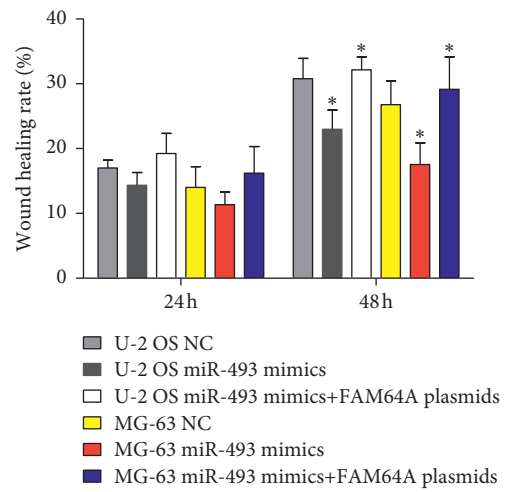
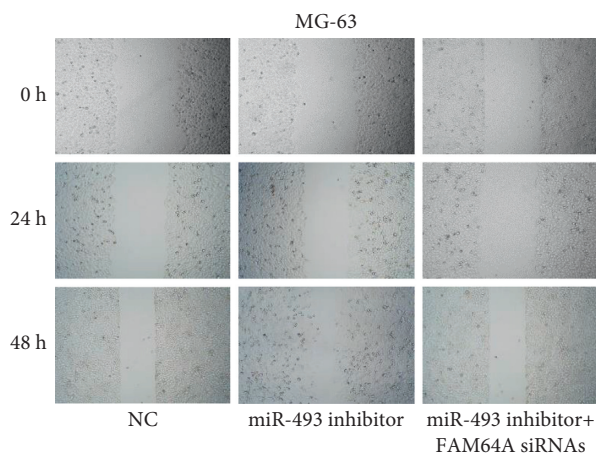


FIGURE 6: Continued.



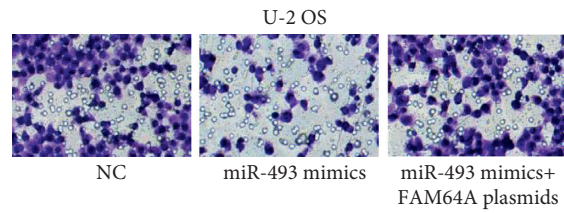
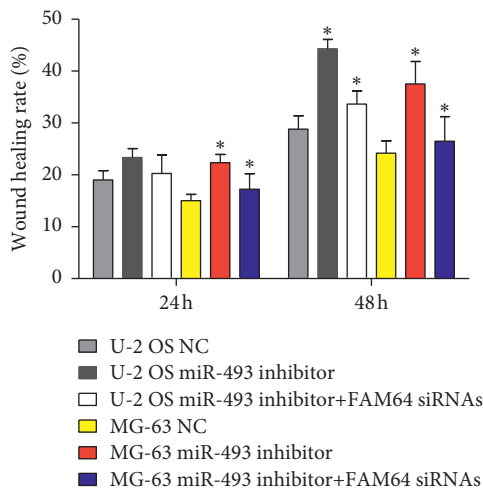
(f)

(g)



(h)

(i)



(j)

(k)

FIGURE 6: Continued.

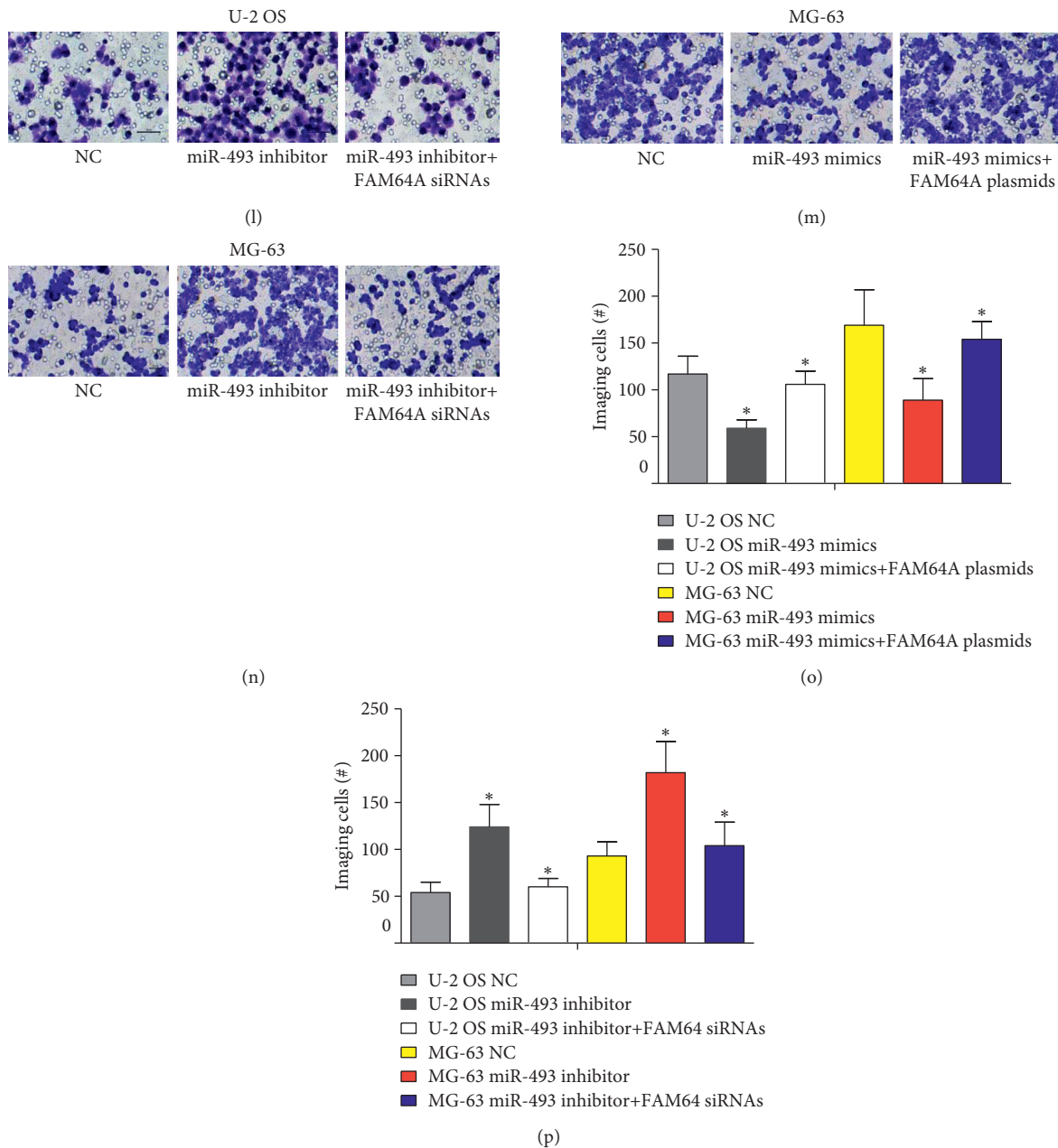


FIGURE 6: miR-493 inhibits proliferation, migration, and invasion of OS cells via regulating FAM64A. (a–p) U-2 OS and MG-63 cells were transfected with miR-493 mimics and miR-493 inhibitors with FAM64A plasmids and FAM64A siRNAs. (a–d) Proliferation of tumor cells was determined by CCK-8 assay. (e–j) Migration was measured by wound healing assay. (k–p) Invasion of cells were analyzed using a Transwell assay. * $P < 0.05$.

Taken together, our data demonstrated that miR-493 negatively regulates FAM64A via binding to its 3' UTR in OS. Our study found that higher expression of FAM64A *in vitro* and *in vivo* is correlated with poor survival in OS. This is the first study to shed light on the participation of FAM64A regulated by miR-439 in the malignancy of osteosarcoma.

Data Availability

The data and materials used to support the findings of this study are included within the published article.

Conflicts of Interest

The authors declare that they have no conflicts of interest.

Acknowledgments

This work was supported by grant NSFC81300346 from the National Natural Science Foundation of China. The data and materials used to support the findings of this study are included within the published article.

References

- [1] C. D. M. Fletcher and K. K. Unni, "Pathology and genetics of tumours of soft tissue and bone," in *World Health Organization Classification of Tumours*, F. Mertens, Ed., IARC Press, Lyon, France, 2002.
- [2] I. Barbutti, J. M. Xavier-Ferrucio, J. A. Machado-Neto et al., "CATS (FAM64A) abnormal expression reduces clonogenicity of hematopoietic cells," *Oncotarget*, vol. 7, no. 42, pp. 68385–68396, 2016.
- [3] C. H. Lin, T. Ji, C.-F. Chen, and B. H. Hoang, "Wnt signaling in osteosarcoma," *Advances in Experimental Medicine and Biology*, vol. 804, pp. 33–45, 2014.
- [4] J. Yan, Q. Wang, K. Zou et al., "Inhibition of the JAK2/STAT3 signaling pathway exerts a therapeutic effect on osteosarcoma," *Molecular Medicine Reports*, vol. 12, no. 1, pp. 498–502, 2015.
- [5] J. Tao, M.-M. Jiang, L. Jiang et al., "Notch activation as a driver of osteogenic sarcoma," *Cancer Cell*, vol. 26, no. 3, pp. 390–401, 2014.
- [6] L. Mei, W. Sang, K. Cui, Y. Zhang, F. Chen, and X. Li, "Norcantharidin inhibits proliferation and promotes apoptosis via c-Met/Akt/mTOR pathway in human osteosarcoma cells," *Cancer Science*, vol. 110, no. 2, pp. 582–595, 2019.
- [7] Z.-S. Xu, H.-X. Zhang, W.-W. Li et al., "FAM64A positively regulates STAT3 activity to promote Th17 differentiation and colitis-associated carcinogenesis," *Proceedings of the National Academy of Sciences*, vol. 116, no. 21, pp. 10447–10452, 2019.
- [8] Z. Zhang, G. Luo, C. Yu, G. Yu, R. Jiang, and X. Shi, "MicroRNA-493-5p inhibits proliferation and metastasis of osteosarcoma cells by targeting Kruppel-like factor 5," *Journal of Cellular Physiology*, vol. 234, no. 8, pp. 13525–13533, 2019.
- [9] M. Qian, H. Gong, X. Yang et al., "MicroRNA-493 inhibits the proliferation and invasion of osteosarcoma cells through directly targeting specificity protein 1," *Oncology Letters*, vol. 15, pp. 8149–8156, 2018.
- [10] J. Zhang, L. Qian, J. Wu et al., "Up-regulation of FAM64A promotes epithelial-to-mesenchymal transition and enhances stemness features in breast cancer cells," *Biochemical and Biophysical Research Communications*, vol. 513, no. 2, pp. 472–478, 2019.
- [11] K. Hashimoto, A. Kodama, T. Honda et al., "Fam64a is a novel cell cycle promoter of hypoxic fetal cardiomyocytes in mice," *Scientific Reports*, vol. 7, no. 1, p. 4486, 2017.
- [12] L. F. Archangelo, P. A. Greif, A. Maucuer et al., "The CATS (FAM64A) protein is a substrate of the Kinase Interacting Stathmin (KIS)," *Biochimica et Biophysica Acta (BBA)—Molecular Cell Research*, vol. 1833, no. 5, pp. 1269–1279, 2013.
- [13] L. F. Archangelo, P. A. Greif, M. Hölzel et al., "The CALM and CALM/AF10 interactor CATS is a marker for proliferation," *Molecular Oncology*, vol. 2, no. 4, pp. 356–367, 2008.
- [14] Y. Gu, Y. Cheng, Y. Song et al., "MicroRNA-493 suppresses tumor growth, invasion and metastasis of lung cancer by regulating E2F1," *PLoS One*, vol. 9, no. 8, Article ID e102602, 2014.
- [15] A. Cui, Z. Jin, Z. Gao et al., "Downregulation of miR-493 promoted melanoma proliferation by suppressing IRS4 expression," *Tumor Biology*, vol. 39, no. 5, 2017.
- [16] K. Ueno, H. Hirata, S. Majid et al., "Tumor suppressor MicroRNA-493 decreases cell motility and migration ability in human bladder cancer cells by downregulating RhoC and FZD4," *Molecular Cancer Therapeutics*, vol. 11, no. 1, pp. 244–253, 2012.
- [17] M. Kleemann, H. Schneider, K. Unger et al., "Induction of apoptosis in ovarian cancer cells by miR-493-3p directly targeting AKT2, STK38L, HMGA2, ETS1 and E2F5," *Cellular and Molecular Life Sciences*, vol. 76, no. 3, pp. 539–559, 2019.

Research Article

Surgical Technique and Outcome of Custom Joint-Sparing Endoprosthesis as a Reconstructive Modality in Juxta-Articular Bone Sarcoma

Ahmad M. Shehadeh ¹, Ula Isleem ², Samer Abdelal,¹ Hamza Salameh ¹
and Muthana Abdelhalim¹

¹Department of Orthopedic Oncology, King Hussein Cancer Center, Queen Rania Street, Amman, Jordan

²Faculty of Medicine, University of Jordan, Queen Rania Street, Amman, Jordan

Correspondence should be addressed to Ahmad M. Shehadeh; ashehadeh@khcc.jo

Received 27 June 2019; Accepted 13 September 2019; Published 26 December 2019

Academic Editor: Shinji Miwa

Copyright © 2019 Ahmad M. Shehadeh et al. This is an open access article distributed under the Creative Commons Attribution License, which permits unrestricted use, distribution, and reproduction in any medium, provided the original work is properly cited.

Background. Joint-sparing limb salvage surgery (JSLSS) is an advancement in the techniques and concepts of limb salvage surgery, which makes it possible to save not only the limb affected by malignancy but also the adjacent joint and the epiphyseal plate. In the growing child, this procedure is technically demanding due to the availability of small length of bone for implant purchase. Reconstruction options can be biological reconstruction or endoprosthesis; however, the outcome of endoprosthetic reconstruction after joint-sparing resection is not well described in the literature. **Purposes.** (1) To determine the prosthesis survival rates when using customized Joint-Sparing Endoprosthesis (JSE) after juxta-articular resection of bone tumors, (2) to investigate the rates of local recurrence, (3) to evaluate the need for revision surgery, and (4) to compare the outcome of customized JSE with that of joint-sacrificing techniques. **Methods.** In our study, joint sparing is defined as any procedure where a custom-made JSE is used in lieu of sacrificing the adjacent joint whenever the length of the remaining bone segment is not enough to accommodate the stem of a modular implant. Twenty-eight patients received JSE, and 31 joints were spared. Their age ranged from 4 to 55 years with a median age of 13 years. Twenty-one patients received surgery for primary reconstruction and 7 patients for revision of failed bone allograft or modular implant. Twenty-four joints are spared in the lower limbs and 7 in the upper limbs. Osteosarcoma was the most common pathological diagnosis ($n = 13$). Flat surface HA-coated custom JSE was used to spare 15 joints, and short-stemmed custom JSE was used to spare 16 joints. The length of the remaining bone epiphysis for JSE anchorage from the knee and ankle joints was 25–75 mm, median = 45 mm, and the length of the cortical bone remaining for the proximal femur and distal humerus was 5–70 mm, median = 10 mm. **Results.** Operative time was 2.5 to 4 hours (avg. 3 hr.) The bone resection surface fitted the prosthesis surface with <2 mm difference. Histological examination of all resected specimens shows clear bone resection margins; 2 patients had positive soft tissue margins. At mean follow-up period of 3 years (6 months–10 years), 6 patients developed local and systemic recurrences, three of them had a pathological fracture at the time of diagnosis ($P = 0.139$), and 4 showed a poor response to chemotherapy ($P = 0.014$); all recurrences occurred in the soft tissue. Implant survival at 5 years was 86.15%, and MSTS score was 90% (83–96%). **Conclusions.** Whenever this kind of implant is affordable and can be utilized, particularly in younger age groups, JSE may be a good reconstruction option to avoid the use of expandable implants and to avoid the potentially higher revision and complication rates associated with biological reconstruction, as well as the complications of conventional joint-sacrificing implant, mainly dislocations and polyethylene wear and tear.

1. Introduction

Joint-sparing limb salvage surgery (JSLSS) is defined as the retention of the native joint in adults and the epiphyseal plate in children when resecting a juxta-articular bone sarcoma. Most patients of bone sarcoma are adolescents and young adults [1]. Furthermore, there are longer survival rates associated with current multidisciplinary treatment modalities. These factors increase the importance of limb and joint salvage in these patients.

Sparing the native joints and epiphyseal plate has several advantages. Preservation of the native joint and all attached ligaments can lead to better proprioception [2], fewer complications related to polyethylene liners of the artificial joints, possible preservation of growth potential, and a decreased need for expandable implants. Preservation of important tendinous attachments can also facilitate rehabilitation and subsequent function.

The challenge in these patients has been to use construct that can reliably grip and hold the small joint- or physis-containing fragment [3]. Reconstruction options after joint-sparing resection of juxta-articular bone sarcoma can be biological (bone allograft and autograft) versus customized joint-sparing implants. The outcome of reconstruction using custom-made Joint-Sparing Endoprosthesis (JSE) is not well described in the literature. A thorough review of the literature shows that only a few papers discussed the outcome of using custom-made implants, with a handful number of patients in each [3–6]. In this paper, we investigate the outcome of using custom JSE in 28 patients and 31 joints, the largest series investigating the outcome of custom JSE in the literature, so far.

The purposes of this study, therefore, were (1) to determine the 5-year survival when using customized Joint-Sparing Endoprosthesis (JSE) after juxta-articular resection of bone tumors, (2) to investigate the rates of local recurrence, (3) to evaluate the need for revision surgery, and (4) to compare the outcome of customized JSE with that of joint-sacrificing techniques.

2. Methods

This retrospective study was conducted at the King Hussein Cancer Center, the only comprehensive cancer center in Jordan.

In our study, joint sparing is defined as any procedure where a custom-made JSE is used in lieu of sacrificing the adjacent joint, in cases where the remaining bone after tumor resection cannot accommodate the stem of a modular implant.

As a reconstructive modality for the resected diaphyseal-metaphyseal segment of bone, we used custom-made JSE, which can have one of the two following designs.

The first design is flat surface hydroxyapatite- (HA-) coated titanium implants, which corresponds neatly to the dimensions and shape of the metaphyseal-epiphyseal residual bone surface. This design is used whenever we have less than 3 cm of cortical bone remaining, and the fixation will be based mainly on the metaphyseal-epiphyseal bone segment. These implants are provided with 2 to 3 HA-

coated, fenestrated fins to maximize bone integration into the metal surface and act as anchorage tool of the implant to the remaining bone segment. These designs are always cementless. They are also equipped with 2-3 HA-coated side plates that are important to prevent angulation while bone ingrowth is still in progress. Construct stability will depend on the successful osseointegration between the implant and the remaining bone (Figure 1).

The second design is cemented short-stemmed implants, where the stem can be either a straight short stem with cross screw(s) or a curved banana shaped stem in proximal femur cases. This design is utilized in cases where the residual cortical bone (diaphyseal bone) is at least 3 cm in length. Both of these are provided with HA-coated side plate(s) that will prevent rotation and stem toggling, and all these stems are fixed with bone cement (Figure 2).

The other side of both implants is fixed to the diaphyseal bone by a cemented or cementless stem; all implants come in 2 pieces: one piece fixed to the metaphyseal-epiphyseal segment of bone, and the other piece fixed to the tubular diaphysis side. Next, both pieces are connected to each other by male-female side mechanism and locked with 2 screws (Figure 3).

2.1. Surgical Protocol. Magnetic resonance images and computerized tomography scans for the affected limb are reviewed thoroughly and carefully by the operating surgeon and radiologists. All distal femurs, proximal tibias, distal tibias, and proximal humeri with a residual bone of more than 25 mm from the articular surface, after tumor resection with at least a 1.5 cm safety margin, were considered eligible to receive joint-sparing resection and JSE reconstruction (Figure 4(a)). All proximal femur segments with 5 mm or more cortical subtrochanteric bone remaining after tumor resection with at least a 1.5 cm safety margin were considered eligible for proximal femur JSE, and all distal humerus segments with 3 cm or more remaining cortical bone above the olecranon fossa were considered eligible for distal humerus JSE (Figures 4(b) and 4(c)).

The MRI and CT scans are sent to the manufacturer (Stanmore Implants Worldwide Ltd, Middlesex, UK) along with our measurements for resection and residual bone length, as well as our design concepts (Figure 5). Afterward, we receive the design proposal for review. If no modifications are needed, then we approve the proposal and wait 6 weeks to have the implant delivered to our hospital.

2.2. Surgical Technique. After general anesthesia, positioning of the patient and prophylactic antibiotics are given. The skin incision is made, creating two flaps. After the release of soft tissue attachments, as well as identification and protection of related major neurovascular structures, a 3D printed cutting guide is held to the surface of the bone harboring the tumor (Figure 6).

Proximal and distal osteotomies through the cutting guide slots are performed. After harvesting bone marrow tissue samples from the proximal and distal bone margin, they are sent for frozen section. Next, we completely resect the specimen (Figure 7).

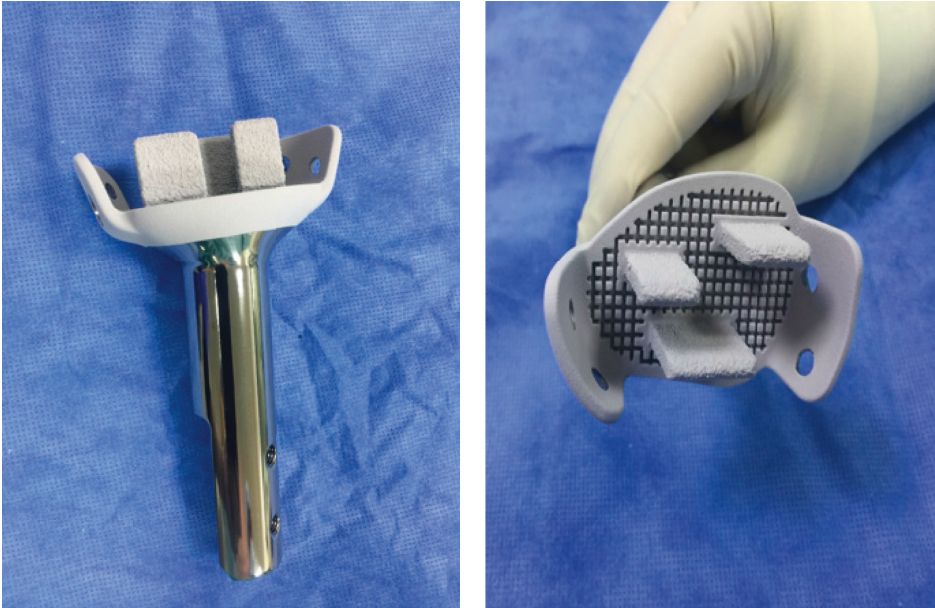


FIGURE 1: Flat surface custom JSE with 3 HA-coated fins and 2 side plates.

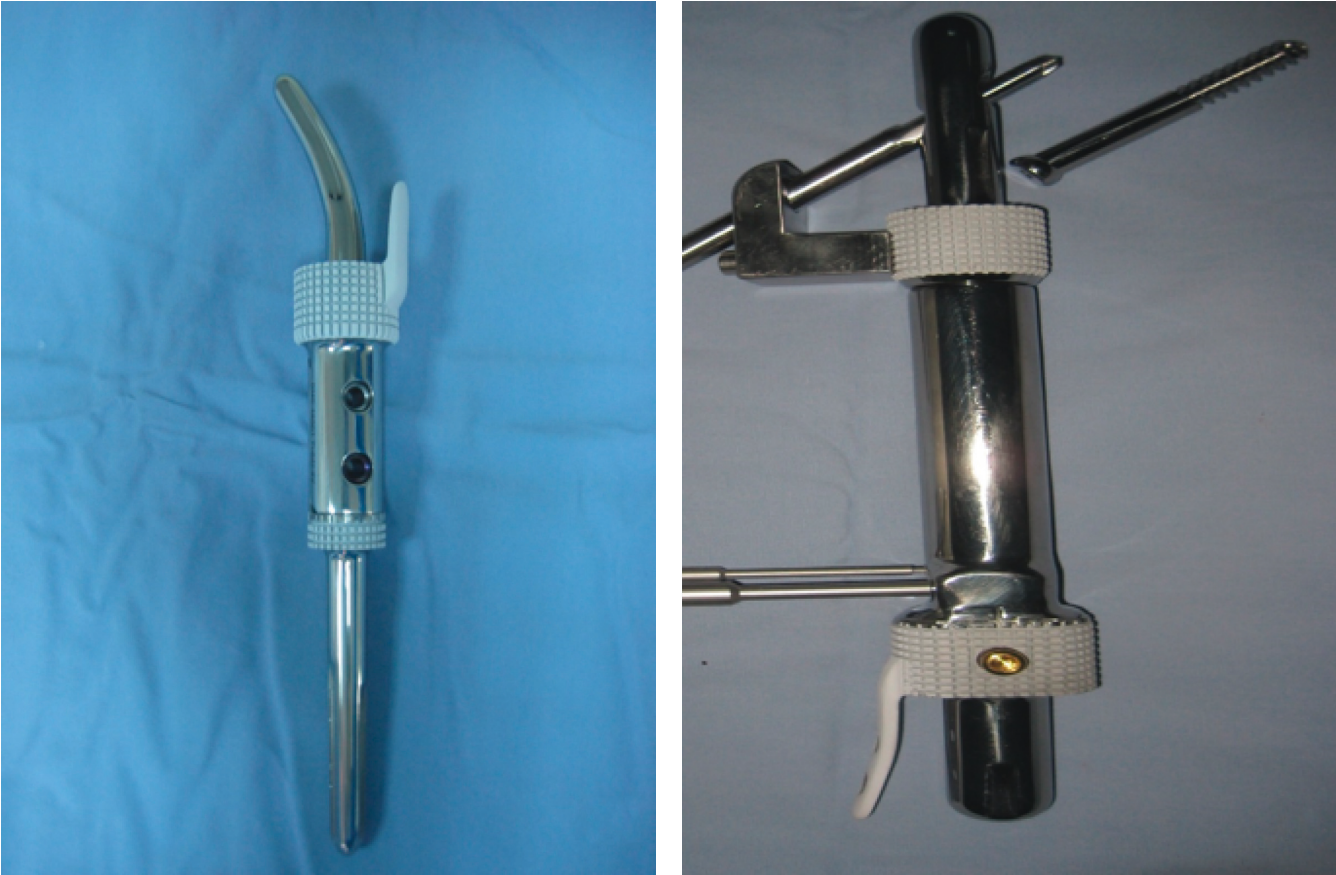


FIGURE 2: (a) Custom JSE with curved stem and HA-coated side plate suitable for proximal femur. (b) Custom JSE for proximal femur and distal femur with cross screw, and one side plate for the distal femur side.

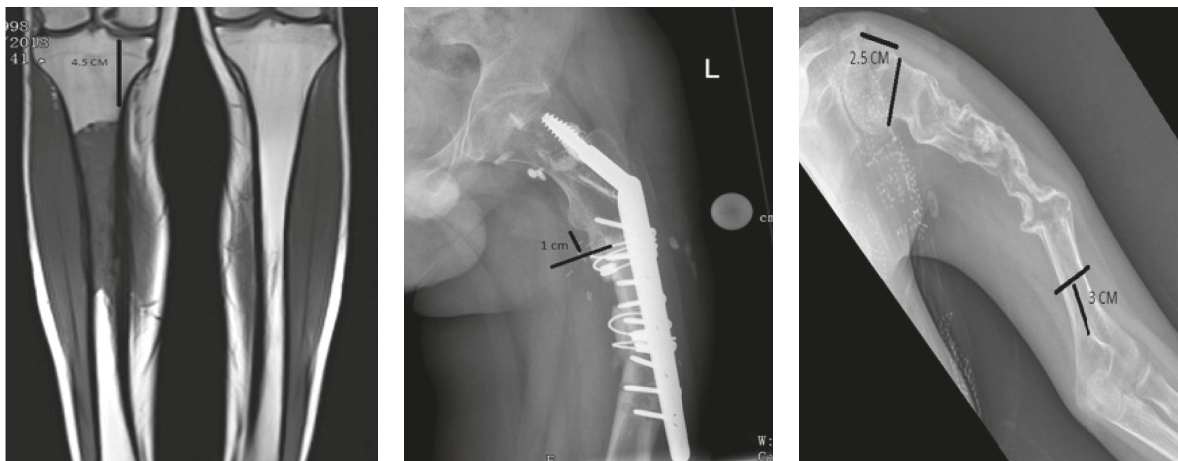


(a)



(b)

FIGURE 3: The 2 parts of the JSE and 2 connecting screws. (a) Before assembly. (b) After assembly.



(a)

(b)

(c)

FIGURE 4: (a) MRI of right tibia of patient with a tibial osteosarcoma, with 4.5 cm remaining length for anchorage of JSE after resection of the tumor with negative margin. (b) Left proximal femur X-ray of a failed bone allograft and DHS cut-off, with 1 cm of cortical bone remaining below the lesser trochanter. A JSE can be used here to revise this failed bone allograft. (c) Left humerus X-ray of postchemotherapy humerus osteosarcoma, showing a 3 cm of cortical bone remaining above the olecranon fossa which makes the sparing of the elbow joint possible. Furthermore, 2.5 cm of bone is remaining proximally making the sparing of the glenohumeral joint possible.

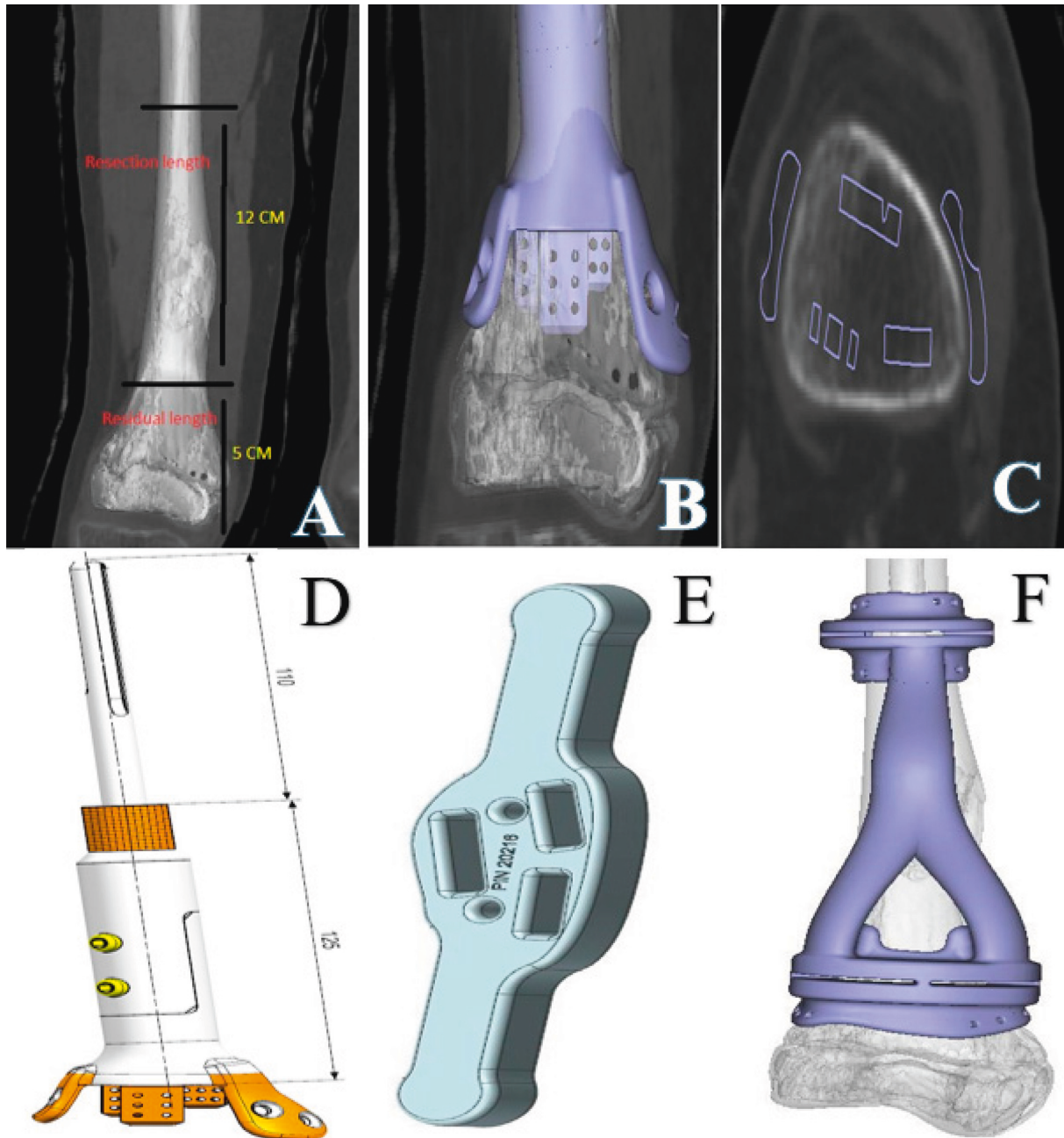


FIGURE 5: (a) A measuring CT scan of femur showing the resection length and residual metaphyseal-epiphyseal bone segment length. (b, c) Fitting of the implant design into the residual bone segment. (d) The final JSE design. (e) The 3D printed fin template which will match in size and dimensions to the metaphyseal surface of residual bone. (f) The 3D printed cutting guide which will be used to make distal and proximal bone osteotomies.

Preparation of the metaphyseal-epiphyseal bone segment is done using a fin template guide and an impaction tool under image intensifier control (Figure 8). After implantation of the joint-saving endoprosthesis, we check the position again under image control and then fix the implant to the epiphyseal bone segment with screws through the side plate (Figure 9).

The second piece of the implant is fixed to the other side of the host bone using a cemented or cementless stem. Finally, both parts of the implant are assembled using locking screws (Figure 10).

Soft tissue coverage of the implant is performed, drains are inserted, and then the incision is closed in layers. Splinting using back slabs is recommended to provide extra stability to the construct and prevent the patient from premature weight bearing.

2.3. Rehabilitation and Aftercare. In all patients with flat surface JSE, where the fixation mechanism is based on successful osseointegration between the implant and the

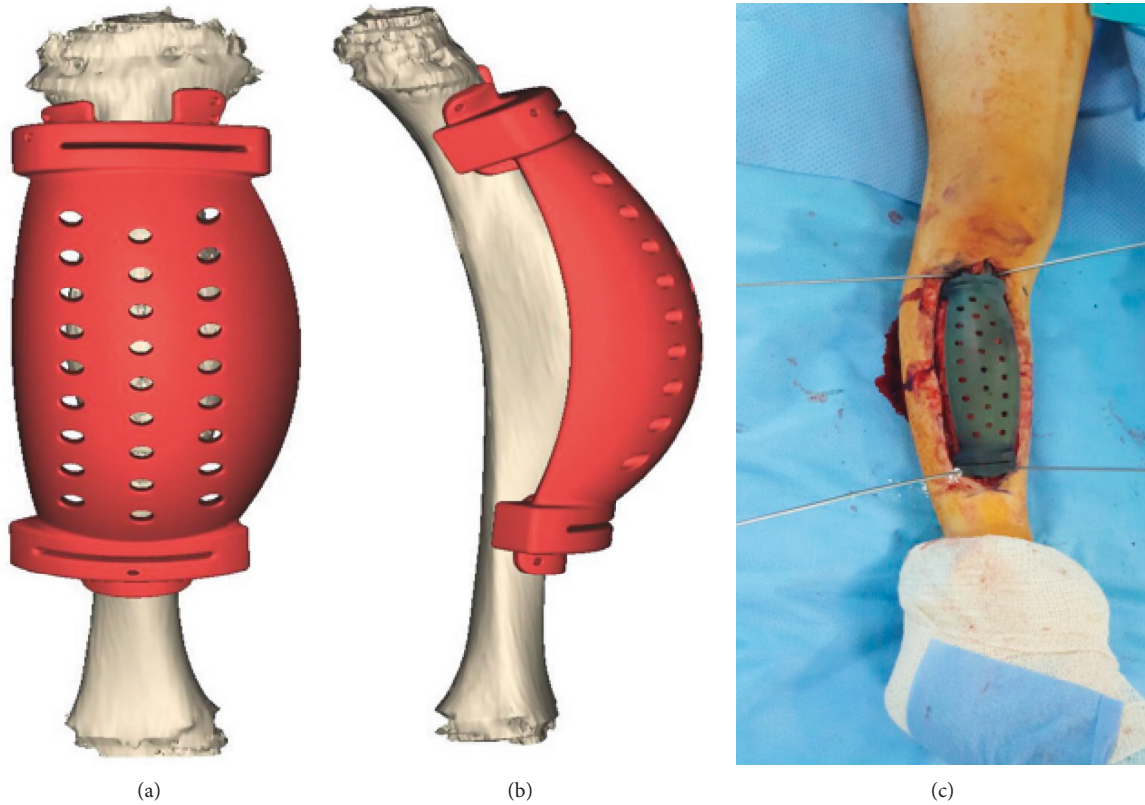


FIGURE 6: (a, b) The 3D printed cutting guide for tibia. (c) The fixation of the 3D printed cutting guide to the patient's tibia using k-wires.

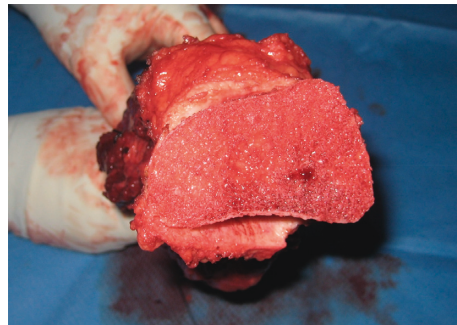


FIGURE 7: The resection specimen showing the metaphyseal cut surface.

bone, the operative limb is kept in an external splint and protected from weight bearing for 8–12 weeks. In patients with a short-cemented stem, they started full weight bearing, as tolerated, at first day postoperatively.

3. Results

A total of 28 patients received custom JSE, 21 of them for primary reconstruction and 7 patients for the revision of a failed bone allograft or modular implant. Thirty-one joints were spared: distal femur ($n=9$), proximal tibia ($n=8$), proximal femur ($n=6$), distal humerus ($n=4$), proximal humerus ($n=2$), and distal tibia ($n=2$).

Of the 7 patients who received JSE for revision, 2 of them had limb-length discrepancy, which prompted the use of an

expandable JSE. The expansion was successfully performed at 5 cm and 9 cm for the two patients. The ages of the patients ranged from 4 to 55 years, with a median age of 13 years. Osteosarcoma was the commonest histological diagnosis Table 1.

3.1. Survival Rates and Complications of the Custom Joint-Sparing Endoprosthesis. Operative time was found to be 2.5–4 hours (with an average of 3 hours). The bone resection surface was fitted to the prosthesis surface with a difference of <2 mm in all dimensions, indicating accuracy of the osteotomies' level. All bone resection margins were free of tumor. Two patients had tumor-positive soft tissue margins.

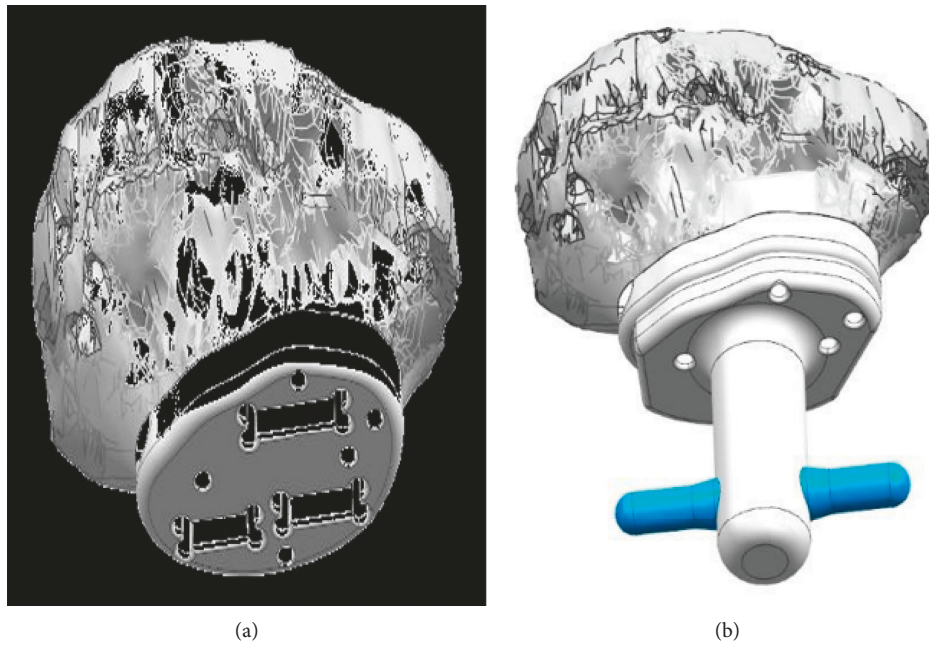


FIGURE 8: (a) Diagram showing the application of fin template to the residual bone surface. (b) The use of the impaction tool to prepare the fin tracks.



FIGURE 9: Intraoperative image intensifier for the position of the implant in the metaphyseal bone segment. (a) Lateral view. (b) AP view.

Implant survival at 3 and 5 years was 88.44 and 86.15%, respectively. (Figure 11).

Twenty-seven of the joints did well with no further operative intervention. Growth of the remaining epiphyseal segment was observed in serial radiological follow-up in all 6 skeletally immature patients who received JSE around the knee joint, with no limb-length discrepancy (Figure 12).

Two patients with flat surface JSE developed failure of osseointegration and loosening of the implant, both with proximal tibia JSE, 4 and 6 months postoperatively, respectively. Clinically, the patients presented with pain on weight bearing. Radiologically, their X-rays show angulation of the implant with a radiolucent line around the fins. Both of them received revision surgery with a new flat surface JSE and did well at the last follow-up (Figure 13). One patient

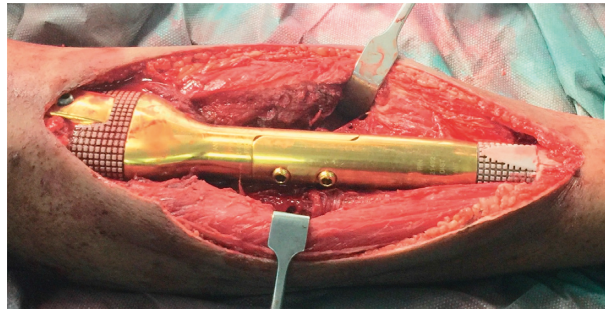


FIGURE 10: Completion of assembly of the 2 sides of the JSE using 2 connecting screws.

TABLE 1: The histological diagnosis of all patients in this study.

Histological diagnosis	Number of patients
Osteosarcoma	13
Ewing sarcoma	10
Adamantinoma	3
Gorham’s disease	1
Myoepithelial carcinoma	1

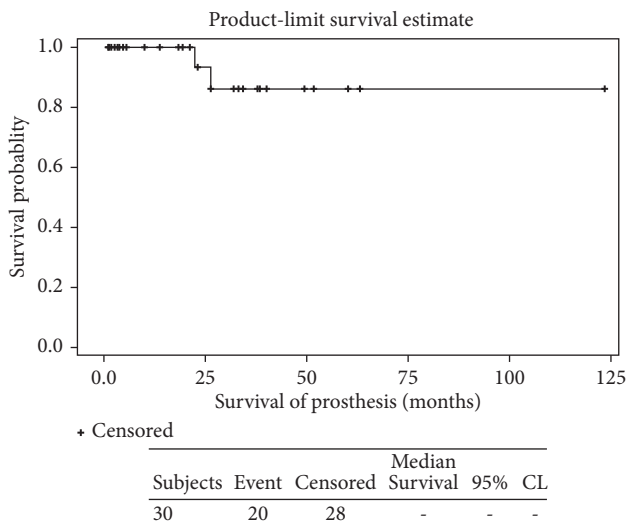


FIGURE 11: The Kaplan–Meier survival curve analysis of all 28 JSE used: the 3-year survival rate: 86.15%; 5-year survival rate: 86.15%.

with a cemented short stem JSE of distal femur, developed loosening but died of systemic disease before revision (Figure 14). The median-modified MSTS score measured 6–12 months after surgery was 90% (83–96%). None of the patients developed joint contractures.

3.2. Local Recurrence Rates of the Tumor. Out of the 24 patients (21 were reconstructed with JSE, and 3 with bone allograft and revised later with JSE) who received joint-sparing surgery for primary tumor reconstruction, 6 developed local recurrences (25%). All recurrences occurred in the soft tissue, with none occurring in the residual bone

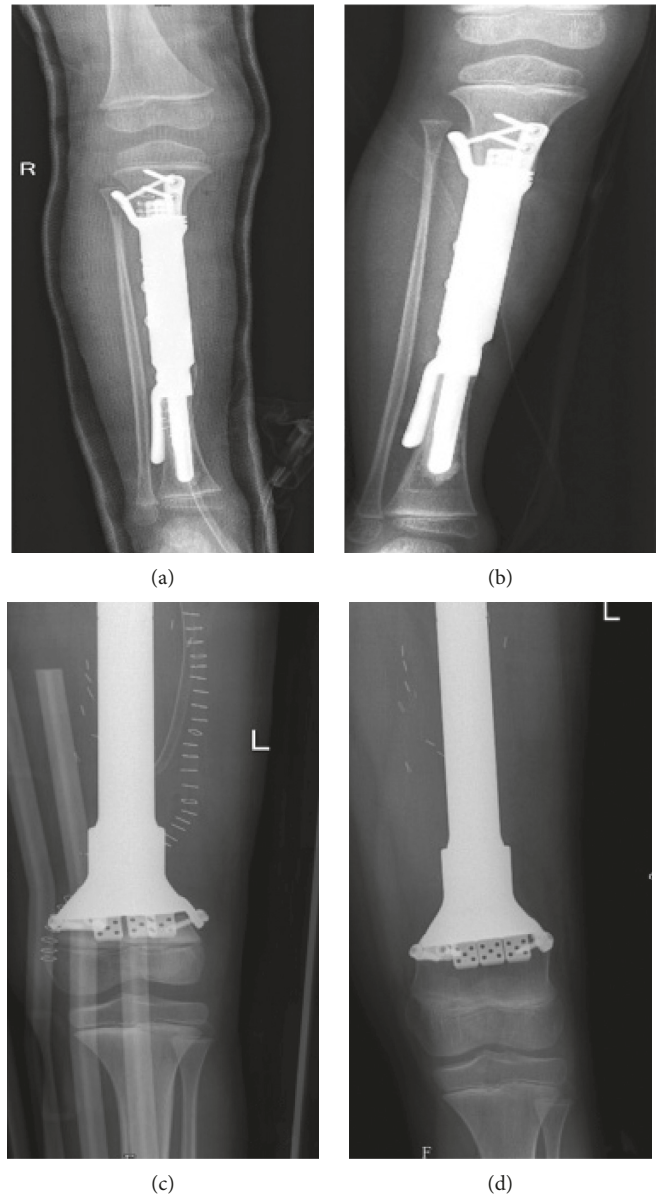


FIGURE 12: (a) Proximal tibia JSE immediately postoperatively and (b) one year after surgery showing the growth of the proximal tibia segment. (c) Distal femur JSE immediately postoperatively and (d) one year after surgery, showing the growth of the distal femur segment.

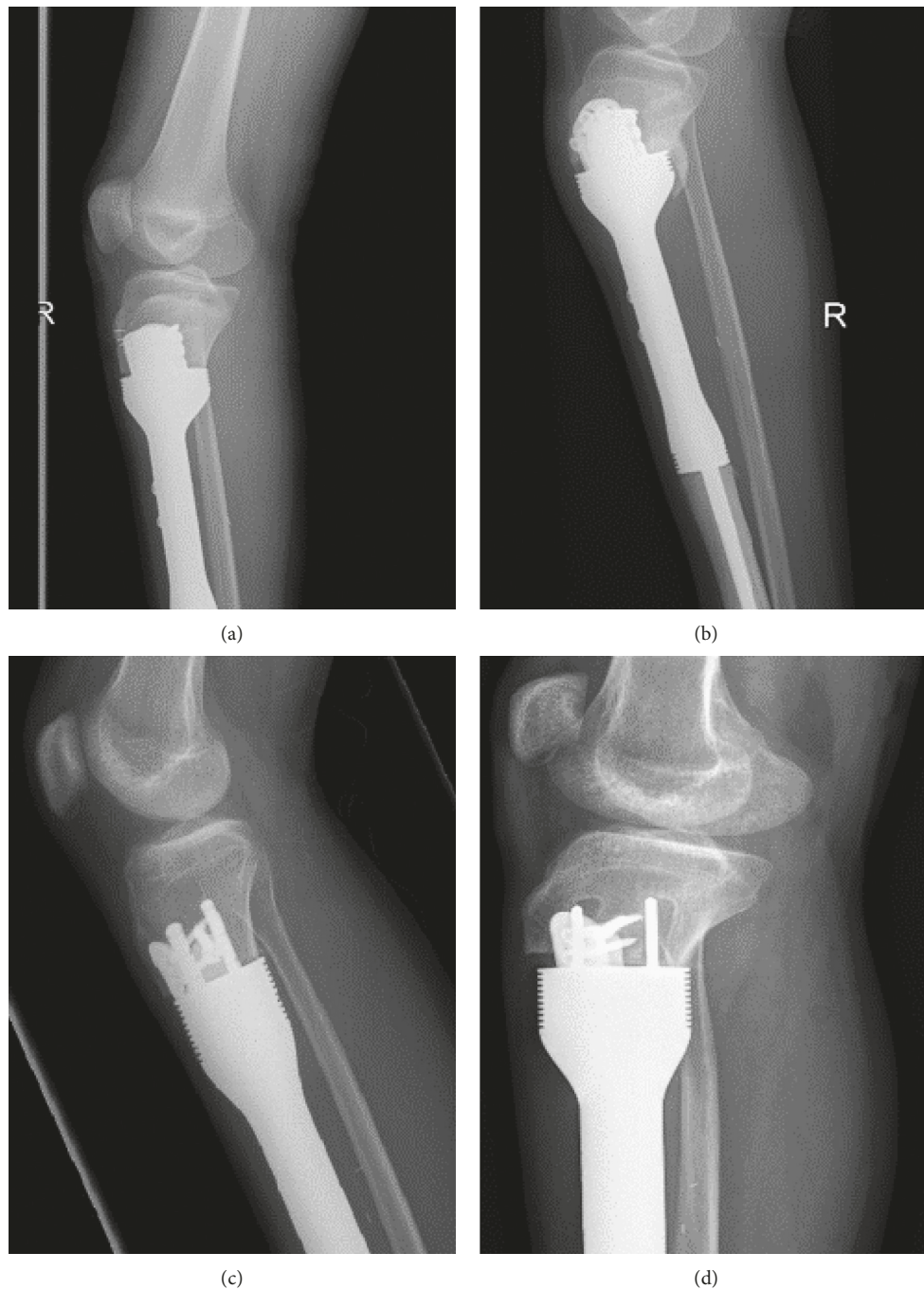


FIGURE 13: Proximal tibia JSE (a) immediately after surgery and (b) 8 months later, with tilting of the proximal metaphyseal tibia segment, and extra cortical bone formation indicating loosening of the implant and failure of osseointegration. (c) Proximal tibia JSE in another patient immediate after surgery and (d) 6 months later, with tilting of the proximal metaphyseal tibia segment, and radiolucent pockets around the fins, indicating failure of osseointegration mechanism.

segment. Three of those with local recurrence had pathological fractures ($P = 0.139$) and 4 showed a poor response to chemotherapy ($P = 0.014$). One of them had positive soft tissue margin ($P = 0.446$) and 4 of them had systemic recurrence Table 2.

Two of them were treated with amputation, two received resection of the soft tissue mass, and two died of systemic recurrence and did not receive surgery for the local recurrence.

Limb survival was 88.44% at 3 years and 86.15% at 5 years (Figure 15).

3.3. Periprosthetic Fracture. One patient with proximal tibia JSE sustained a periprosthetic fracture at the distal cemented stem and received fixation with plate and screws (Figure 14).

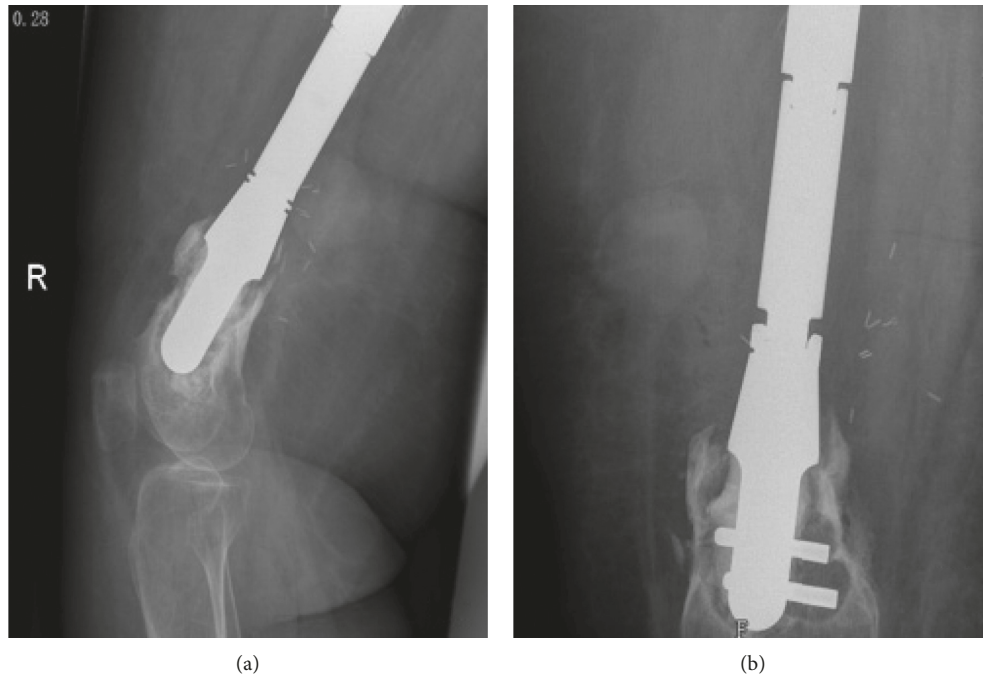


FIGURE 14: (a) Lateral and (b) AP films of distal femur cemented JSE, 2 years after surgery, showing radiolucent lines and bone destruction of the remaining bone segment.

TABLE 2: The association between tumor recurrence and response to chemotherapy, pathological fracture, and surgical margins.

Factors	Presence/absence	Total	Local recurrence		P value
			Absent	Present	
Pathologic fracture	No	18 (75.0%)	15 (83.3%)	3 (50.0%)	0.139
	Yes	6 (25.0%)	3 (16.7%)	3 (50.0%)	
Response to neoadjuvant chemotherapy (n = 21)	Good response	14 (70.0%)	13 (86.7%)	1 (20.0%)	0.014
	Poor response	6 (30.0%)	2 (13.3%)	4 (80.0%)	
Soft tissue margins	Negative	22 (91.7%)	17 (94.4%)	5 (83.3%)	0.446
	Positive	2 (8.3%)	1 (5.6%)	1 (16.7%)	

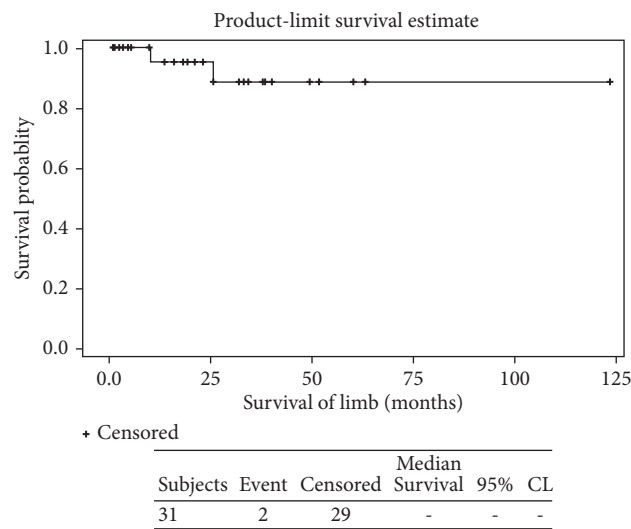


FIGURE 15: The Kaplan–Meier survival analysis of all 28 limbs: the 3-year survival rate was 88.44% and the 5-year survival rate was 86.15%.

TABLE 3: The literature review of joint-sparing limb salvage using biological reconstruction, showing complications and functional outcome.

Series	Year	No. of patients	Implant/allograft and site of the tumor	Survival of the allograft at last follow-up	Complications/revision	Infection	Recurrence	MSTS score
(1) Manfrini et al. [12]	1999	10	Vascularized fibula graft and massive allograft		Valgus deformity limb-length discrepancy 2–3.5 cm	None reported	None reported, but 4 were lost for follow-up	Satisfactory
(2) Aponte-Tinao et al. [7]	2015	35	Epiphyseal preservation and allograft tibia and femur	Overall survival rate of the patients was 86% at 5 years	14 (40%) patients Fracture and nonunion. Removal in 10 patients	2 (6%)	3	The mean functional score was 26 points at final follow-up
(3) Agarwal et al. [3]	2010	19	Bone allograft, autograft, or vascularized fibula	16/25 at a median follow-up of 34 months. There were four deaths	4 (22%) fracture and nonunion	2 (10%)	4	The musculoskeletal tumor society score ranged from 27 to 30
(4) Abdelaal et al. [9]	2015	18	Epiphyseal sparing and reconstruction	Five- and ten-year rates of survival were 94.4%	Fracture of the graft and nonunion in 2 patients (11%)	2 (11%)	1	MSTS score was excellent in 17 patients (94.4%) and poor in one (5.5%)
(5) Li et al. [11]	2017	41	Vascularized fibula and bone allograft	All at follow-up of 3–11 years Mean 4.4 years	Revision in 10 patients (24%) osteonecrosis in remaining epiphysis in 13 patients. (31%)		3	MSTS score 22–30 Median = 28
(6) Muratori et al. [13]	2018	64	Resections around ankle, knee, and hip	Mean follow-up was 117 months (12–305)	Fracture 26%. Nonunion 14%	3 patients (4.7%)	Not reported	27 (18–30)

TABLE 4: The literature review of joint-sparing limb salvage using JSE for reconstruction, showing complications and functional outcome.

Series	Year	No. of patients	Implant/allograft and site of the tumor	5 year survival of the implant or the allograft or last follow-up	Complications/revision	Infection	Recurrence	MSTS score
(1) Gupta et al. [4]	2006	8	Knee-sparing distal femoral endoprosthesis	Mean follow-up: 24 months	0	1 patient developed septicemia two weeks after surgery	0	The mean was 80% (57% to 96.7%)
(2) Agarwal et al. [3]	2010	6	Custom implant prosthesis	Mean follow-up: 12–27 months 1 patient died	0	2 deep infection	1	The score ranged from 27 to 30
(3) Wong et al. [6]	2013	8	6 femur, 1 tibia, and 1 proximal humerus Stanmore	Mean follow-up: 41 months	0	0	0	The mean score was 29.1 (range, 28–30)
(4) Spiegelberg et al. [5]	2009	8	proximal tibia replacement epiphyseal sparing	The mean follow-up: 35 months	1 periprosthetic fracture	0	1 converted to BKA	The mean score was 24 of 30 79% (57% to 90%)
This study	2019	28	Custom Joint-Sparing Endoprosthesis (JSE), from Stanmore	The mean follow-up: 3 years	3 loosening 2 of them revised with new JSE	0	6, 2 of them received AKA	The mean score was 90% (83–96%)

4. Discussion

Joint sparing has many advantages as mentioned previously; however, it also comes with many challenges. The main challenge is finding the appropriate reconstruction modality. A thorough review of the literature shows that most of the case series employed biological reconstruction. The outcome of biological reconstruction is associated with a higher incidence of failure, due to fracture, nonunion, and infection, in addition to the long operative time needed, especially when utilizing vascularized fibulas. There was also a frequent need for revision surgery as well as, prolonged protected weight bearing after surgery and longer rehabilitation. The incidence of all major complications encountered in biological reconstruction ranges from 32 to 47% [2, 7–13], with similar revision rates. Furthermore, in many techniques used in bone allograft reconstruction, the fixation plate will cause premature epiphysiodesis and early closure of the epiphyseal plate, with no attempt at preserving the growth potential of the growing bone and subsequent need for bone elongation procedures Table 3 [7].

The use of custom-made JSE is previously described in the literature [3, 4]. The complications associated with this approach were deep infection and periprosthetic fractures, but no limb loss for implant-related complications; however, the number of patients included in previously reported papers regarding JSE is relatively small.

In this study, we report the outcome of 28 patients receiving custom JSE, the biggest series on this topic, to date.

Three of our patients developed implant-related complications and 6 developed local recurrences, which was found to be related significantly to poor response to chemotherapy in the subgroup of patients who received this surgery, rather than the surgery itself ($P < 0.05$).

When comparing the complications and the revision rate in this series to others using a bone allograft, a lower complication rate was found and operative time was shown to be shorter (Table 4). When compared to joint-sacrificing approaches, there was no increased incidence of local recurrence or implant-related complications. Furthermore, the functional outcome was found to be favorable, with our study showing an MSTS score of 90%.

After reviewing the survival rates and complications of conventional joint-sacrificing endoprosthesis, Shehadeh et al. [14] studied the outcome of endoprosthesis in 232 patients. The total complication rate was 41%, the revision rate of the implants was 29%, and the infection rate was 13%. The 5-year survival of modular and custom-made implants was 85% and 79%, respectively. Comparing our results to those results shows a favorable outcome, with a 5-year survival rate of 86% in our study.

One of the limitations of this study is the fact that this is a retrospective study over a relatively short duration. Although this study has the largest sample size, the patient population is still too small to draw any firm conclusions or to compare outcomes between different anatomical locations. In addition, there is no comparison with control groups with biological reconstruction and conventional joint-sacrificing approach.

Nonetheless, our study outcomes show that the use of JSE in joint-sparing limb salvage surgery is a safe reconstruction modality with no increased risk of complications and does not jeopardize the oncological principles for bone tumors surgery.

5. Conclusion

Whenever this kind of implant is affordable and can be utilized, particularly in younger age groups, JSE may be a good reconstruction option to avoid the use of expandable implants and to avoid the potentially higher revision and complication rates associated with biological reconstruction, as well as the complications of conventional joint-sacrificing implant, mainly dislocations and polyethylene wear and tear.

Data Availability

The data used to support the findings of this study are included within the article.

Conflicts of Interest

The authors declare no conflicts of interest.

References

- [1] Z. Burningham, M. Hashibe, L. Spector, and J. D. Schiffman, "The epidemiology of sarcoma," *Clinical Sarcoma Research*, vol. 2, no. 1, p. 14, 2012.
- [2] S. M. Kumta, T. C. Chow, J. Griffith, C. K. Li, J. Kew, and P. C. Leung, "Classifying the location of osteosarcoma with reference to the epiphyseal plate helps determine the optimal skeletal resection in limb salvage procedure," *Archives of Orthopaedic and Trauma Surgery*, vol. 119, no. 5-6, pp. 327–331, 1999.
- [3] M. Agarwal, A. Puri, A. Gulia, and K. Reddy, "Joint-sparing or physeal-sparing diaphyseal resections: the challenge of holding small fragments," *Clinical Orthopaedics and Related Research*, vol. 468, no. 11, pp. 2924–2932, 2010.
- [4] A. Gupta, R. Pollock, S. R. Cannon, T. W. R. Briggs, J. Skinner, and G. Blunn, "A knee-sparing distal femoral endoprosthesis using hydroxyapatite-coated extracortical plates," *The Journal of Bone and Joint Surgery. British Volume*, vol. 88-B, no. 10, pp. 1367–1372, 2006.
- [5] B. G. I. Spiegelberg, M. D. Sewell, W. J. S. Aston et al., "The early results of joint-sparing proximal tibial replacement for primary bone tumours, using extracortical plate fixation," *The Journal of Bone and Joint Surgery. British Volume*, vol. 91-B, no. 10, pp. 1373–1377, 2009.
- [6] K. C. Wong and S. M. Kumta, "Joint-preserving tumor resection and reconstruction using image-guided computer navigation," *Clinical Orthopaedics and Related Research*, vol. 471, no. 3, pp. 762–773, 2013.
- [7] L. Aponte-Tinao, M. A. Ayerza, D. L. Muscolo, and G. L. Farfalli, "Survival, recurrence, and function after epiphyseal preservation and allograft reconstruction in osteosarcoma of the knee," *Clinical Orthopaedics and Related Research*, vol. 473, no. 5, pp. 1789–1796, 2015.
- [8] R. S. Avedian, R. C. Haydon, and T. D. Peabody, "Multiplanar osteotomy with limited wide margins: a tissue preserving surgical technique for high-grade bone sarcomas," *Clinical*

- Orthopaedics and Related Research*®, vol. 468, no. 10, pp. 2754–2764, 2010.
- [9] A. Hamed Kassem Abdelaal, N. Yamamoto, K. Hayashi, A. Takeuchi, S. Miwa, and H. Tsuchiya, “Epiphyseal sparing and reconstruction by frozen bone autograft after malignant bone tumor resection in children,” *Sarcoma*, vol. 2015, Article ID 892141, 8 pages, 2015.
- [10] J. Li, L. Shi, and G.-J. Chen, “Image navigation assisted joint-saving surgery for treatment of bone sarcoma around knee in skeletally immature patients,” *Surgical Oncology*, vol. 23, no. 3, pp. 132–139, 2014.
- [11] J. Li, Z. Wang, C. Ji, G. Chen, D. Liu, and H. Zhu, “What are the oncologic and functional outcomes after joint salvage resections for juxtaarticular osteosarcoma about the knee?,” *Clinical Orthopaedics and Related Research*®, vol. 475, pp. 2095–2104, 2017.
- [12] M. Manfrini, A. Gasbarrini, C. Malaguti et al., “Intra-epiphyseal resection of the proximal tibia and its impact on lower limb growth,” *Clinical Orthopaedics and Related Research*, vol. 358, pp. 111–119, 1999.
- [13] F. Muratori, F. Totti, A. D’Arienzo et al., “Biological intercalary reconstruction with bone grafts after joint-sparing resection of the lower limb: is this an effective and durable solution for joint preservation?,” *Surgical technology international*, vol. 1, no. 32, pp. 345–346, 2018.
- [14] A. Shehadeh, J. Noveau, M. Malawer, and R. Henshaw, “Late complications and survival of endoprosthetic reconstruction after resection of bone tumors,” *Clinical Orthopaedics and Related Research*®, vol. 468, pp. 2885–2895, 2010.